

AnyGroundBench: A Specialized-Domain Benchmark for Video Grounding in Vision-Language Models

Rintaro Otsubo^{1,2*} Ryo Fujii^{1,2*} Reina Ishikawa^{1,2} Taiki Kanaya^{1,2} Kanta Sawafuji^{1,2}
 Hiroki Kajita^{1,3} Shigeki Sakai^{1,3} Hideo Saito^{1,2} Ryo Hachiuma⁴
¹Keio University ²Keio AI Research Center ³Keio University School of Medicine ⁴NVIDIA
 *Equal contribution

[Project Page](#) [GitHub](#) [Hugging Face](#)

Abstract

Vision-Language Models (VLMs) have demonstrated immense promise in Spatio-Temporal Video Grounding (STVG). However, current evaluation protocols are largely confined to zero-shot assessments on general, daily-life benchmarks. This creates a critical disconnect from real-world applications in specialized fields, where models inevitably encounter rare visual concepts and complex spatio-temporal dynamics. Since exhaustive pre-training across infinite data distributions is infeasible, the ability to adapt to novel domains is essential. To bridge this gap, we introduce AnyGroundBench, a domain-adaptation benchmark designed to shift the STVG evaluation paradigm from static zero-shot testing to rigorous domain adaptation. Targeting five specialized domains (animal, industry, sports, surgery, and public security), AnyGroundBench pairs newly captured videos such as expert-annotated mouse behaviors with established datasets, unifying them through dense, high-fidelity spatio-temporal annotations. Crucially, the benchmark provides dedicated training subsets to systematically measure domain adaptability. We extensively evaluate 15 state-of-the-art VLMs, assessing their zero-shot generalization and In-Context Learning (ICL) capabilities under practical computational constraints. Ultimately, our findings reveal that current models fail in both zero-shot and ICL-based adaptation when confronted with specialized domains, exposing critical flaws in spatio-temporal reasoning that future research must address.

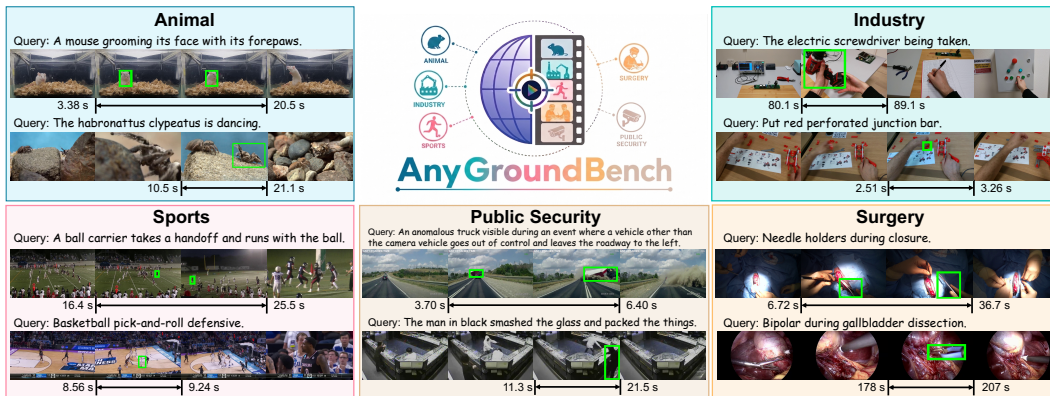


Figure 1: **AnyGroundBench examples across five specialized domains.** AnyGroundBench integrates newly captured, expert-annotated videos with established public datasets, unifying them through dense, new high-fidelity spatio-temporal annotations and language queries.

1 Introduction

Spatio-Temporal Video Grounding (STVG) is one of the critical and fundamental tasks in the video perception field that requires localizing a target object across both spatial and temporal dimensions in the video based on natural language queries. Its importance is underscored by its role in high-stakes applications, such as video retrieval [20], video reasoning [7, 39], and autonomous driving [76]. Recently, the field has transitioned from specialized model architectures [28, 56, 58, 63, 78] toward Vision-Language Models (VLMs) [2, 21, 22, 33, 35, 42, 59, 60, 77]. By incorporating the grounding capability in a single unified model, VLMs can extend this capability to the task which require both perception and reasoning, such as grounded video question answering [64, 53, 69], grounded reasoning [39], and agentic tool-calling [32].

Despite recent progress, most established benchmarks [6, 16, 30, 33, 36, 54, 58, 66, 68, 72, 78] remain predominantly focused on everyday scenarios and general objects. However, real-world deployments inevitably extend beyond such settings. For example, the ability to spatio-temporally localize specific mouse behaviors, such as scratching, is crucial for dermatology or neurology research [50]. In such highly specialized domains, both the visual appearance and the intricate spatio-temporal dynamics deviate significantly from those found in everyday activities. This naturally raises a fundamental question: *Can existing VLMs effectively adapt to ground anything in these uncommon and domain-specific scenarios?*

Addressing this question is hindered not only by the lack of benchmarks for specialized domains but also by evaluation protocols, which rely excessively on zero-shot performance [71]. While VLMs have demonstrated remarkable foundational power, it is practically infeasible for any model to *pre-learn* the near-infinite variety of data distributions encountered (or will be encountered in the future) in the wild. As novel domains and tasks continuously emerge in the real-world, such as the aforementioned laboratory or industrial settings [44, 45], a model’s capability cannot be measured solely by its static pre-trained knowledge. Instead, the ability to seamlessly adapt to a rare domain becomes a strict requirement for real-world deployment. Therefore, to understand whether a model can perceive the data from specialized domains, the evaluation paradigm must shift from testing zero-shot performance to measuring adaptability. Moreover, due to the nature of the data collection difficulty in the specialized domains, the adaptation should be conducted in the *few-shot* manner.

To bridge these two crucial gaps in domain coverage and adaptability evaluation, we introduce **AnyGroundBench** (Figure 1), a domain-adaptation benchmark that shifts the evaluation paradigm for STVG from general zero-shot evaluation to adaptation to specialized domains. AnyGroundBench comprises 2,040 videos as well as natural language queries and corresponding spatio-temporal bounding boxes. AnyGroundBench offers two key advantages. (1) **Diverse and High-Quality Data in Specialized Domains.** AnyGroundBench targets five specialized domains: animal, industry, sports, surgery, and public security. For data sourcing, we aggregate videos from entirely novel captures (including American football from the sports domain and medical expert-curated mouse scratching from the animal domain) alongside new annotations to the public datasets. To ensure high-fidelity annotations, we manually provide dense spatio-temporal bounding boxes for ungrounded videos and transform existing labels for the spatio-temporal grounding task if applicable. (2) **Dedicated Training Sets for Domain Adaptation.** Unlike previous benchmarks that rely exclusively on general-domain training, AnyGroundBench provides tailored training subsets for each domain. This design explicitly enables researchers to systematically evaluate VLMs’ few-shot adaptation capability: how effectively they adjust to the unique spatio-temporal dynamics inherent to specialized fields.

We evaluate 15 VLMs on our benchmarks, including both open-source and closed-source proprietary models with diverse architectures and model sizes. In addition, we further decompose STVG tasks into isolated Spatial Video Grounding (SVG), which focuses on spatial localization within ground-truth time spans, and Temporal Video Grounding (TVG), which targets temporal boundary detection, thereby pinpointing precisely where current spatio-temporal reasoning breaks down. Furthermore, to measure the adaptability of VLMs as a reference for future benchmark users, we employ In-Context Learning [4]—a representative backpropagation-free approach that reflects the strict computational constraints frequently encountered in real-world applications.

We reveal three critical findings about VLMs’ grounding capability in specialized domains:

- **Limited Grounding Capability of Current VLMs:** Even the most advanced proprietary models fail to achieve practical STVG performance, while open-source models exhibit a complete collapse, lacking fundamental spatial reasoning entirely.

- **Spatial Grounding as the Primary Bottleneck:** Dissecting this failure reveals that while temporal grounding shows promise under loose thresholds, spatio-temporal performance completely collapses under practical metrics (*e.g.*, $vIoU@0.5$) due to severe limitations in Spatial Video Grounding.
- **Inconsistent Performance Gain of Inference-time Adaptation:** Attempting domain adaptation via In-Context Learning (ICL) presents a critical instability; depending on the model and domain, while few-shot demonstrations improve temporal localization, they frequently exert a negative impact on grounding accuracy, suggesting the development of a robust adaptation approach.

2 Related Work

Benchmark for Spatio-Temporal Video Grounding. Spatio-temporal video grounding (STVG) aims to localize a target object specified with the text query in both the space and time axes. Progress in this field has been heavily driven by large-scale datasets [6, 30, 36, 66, 68, 72, 78]. Traditionally, benchmarks like VidSTG [78] (built upon VidOR [52]) and HC-STVG [58] (sourced from AVA [19] and YouTube) have served as primary testbeds, focusing mainly on generic objects and human-centric activities. More recently, LLaVA-ST [33] enhanced VidSTG with LLM-generated text queries, and OmniGround [16] was introduced to cover a wider range of object categories by collecting videos from Pexels¹ and RVOS [9, 51].

However, existing benchmarks share a major limitation: owing to their reliance on general internet platforms and existing generic datasets, they remain heavily confined to common daily-life domains. This narrow scope leaves a critical void for evaluating models in highly specialized, real-world scenarios. To bridge this gap, AnyGroundBench explicitly targets specialized fields. Crucially, we differentiate our work by combining *newly captured* videos curated from experts with established domain-specific datasets with unified, high-fidelity annotations. This exclusive combination provides a benchmark for evaluating STVG domain-adaptation capabilities.

Spatio-Temporal Video Grounding via VLMs. Recently, VLMs have dominated not only video understanding tasks [11, 79] but also video perception tasks, such as STVG [2, 35, 33, 59, 60, 77]. Yet, current evaluation protocols for these models rely almost exclusively on zero-shot performance on the general-domain benchmarks [71]. While measuring foundational knowledge is useful, it ignores the reality of real-world deployments. Since it is impossible to pre-train a model on every conceivable domain, practical systems must rapidly adapt to unseen, specialized data. Currently, the field lacks standardized and unified benchmarks designed to explicitly measure domain adaptability (*e.g.*, via In-Context Learning (ICL) [4, 10, 14, 29, 49, 65, 67, 74]). AnyGroundBench is the first benchmark to fill both of these critical gaps by providing highly specialized target domains equipped with standardized adaptation training sets.

3 AnyGroundBench





We introduce AnyGroundBench, a benchmark designed to evaluate STVG capability as well as the adaptation across five specialized domains that present distinct challenges and high real-world relevance: animal, industry, sports, surgery, and public security. To evaluate the adaptability, AnyGroundBench provides training subsets for each domain. An overview of the selected domains and statistics are summarized in Table 1. Details are provided in Appendix C.


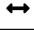
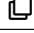

3.1 Benchmark Tasks

AnyGroundBench evaluates models on three interconnected tasks defined over a video and a corresponding text query in a zero-shot and few-shot (adaptation) manner. The same VLM is used across all three tasks; the task is induced solely by a task-specific system prompt. We first introduce a unified notation to formalize each task.

Notation. Let $V = \{I_t\}_{t=1}^T$ denote a video of T frames with $I_t \in \mathbb{R}^{H \times W \times 3}$, and let Q be a natural-language query referring to a target object and its associated event. A per-frame axis-aligned

¹<https://www.pexels.com>

Table 1: **Overview of AnyGroundBench.** Our benchmark emphasizes domain diversity and high-fidelity manual annotations for specialized scenarios. : Newly captured videos, : Temporal span annotation, : Spatial box annotation, : Text query annotation.

Domain	Data Source	# Videos	Avg. Dur. (sec)	# QA Pairs		Additional Efforts			
				Train	Test				
Animal	Animal Kingdom [40]	183	36	475	106			✓	
	Mouse Scratching	103	65	108	51	✓	✓	✓	✓
Industry	MECCANO [44]	169	43	258	111				
	ENIGMA [45]	85	71	152	58			✓	✓
Sports	MultiSports [34]	434	17	374	126				
	American Football	123	30	86	37	✓	✓	✓	✓
Surgery	EgoSurgery [13, 15, 12]	150	61	535	179				✓
	CholecTrack20 [41]	41	143	21	37				✓
Public Security	UCA [75, 57]	43	111	80	19			✓	
	DoTA [73]	709	10	478	231				

bounding box² is written as $b_t \in \mathbb{R}^4$, and a spatio-temporal tube on an interval $[t_s, t_e] \subseteq [1, T]$ as

$$\tau = \left\{ (t, b_t) \right\}_{t=t_s}^{t_e}. \quad (1)$$

Each test instance is paired with a ground-truth tube $\tau^* = \left\{ (t, b_t^*) \right\}_{t=t_s^*}^{t_e^*}$. We denote the evaluated VLM by \mathcal{F}_θ with parameters θ . All three tasks invoke the same \mathcal{F}_θ ,

$$\hat{y} = \mathcal{F}_\theta(V, Q; p), \quad (2)$$

where $p \in \{p_{\text{STVG}}, p_{\text{SVG}}, p_{\text{TVG}}\}$ is the task-specific system prompt (full templates in Appendix B) and \hat{y} is the output type appropriate to the task. The three tasks correspond to estimating different subsets of τ^* from (V, Q) .

Spatio-Temporal Video Grounding (STVG) requires localizing the target object matching the query in both the spatial and temporal axes. Given (V, Q) and the system prompt p_{STVG} , the model predicts the full tube as:

$$\hat{\tau} = \mathcal{F}_\theta(V, Q; p_{\text{STVG}}) = \left\{ (t, \hat{b}_t) \right\}_{t=\hat{t}_s}^{\hat{t}_e}, \quad (3)$$

i.e., both the temporal interval $[\hat{t}_s, \hat{t}_e]$ and the bounding box \hat{b}_t in every frame inside it.

Spatial Video Grounding (SVG) focuses on spatial localization within a temporally trimmed video, isolating the spatial component of grounding from temporal-boundary estimation. Given the trimmed video $V_{[t_s^*, t_e^*]} = \{I_t\}_{t=t_s^*}^{t_e^*}$, the query Q , and the system prompt p_{SVG} , the model predicts a per-frame bounding-box sequence as:

$$\{\hat{b}_t\}_{t=t_s^*}^{t_e^*} = \mathcal{F}_\theta(V_{[t_s^*, t_e^*]}, Q; p_{\text{SVG}}). \quad (4)$$

Temporal Video Grounding (TVG) aims to determine the correct temporal boundaries of the queried event, effectively performing temporal segment localization. Given (V, Q) and the system prompt p_{TVG} , the model predicts only the temporal interval

$$[\hat{t}_s, \hat{t}_e] = \mathcal{F}_\theta(V, Q; p_{\text{TVG}}). \quad (5)$$

3.2 Adaptation Protocol

AnyGroundBench provides per-domain training sets $\mathcal{T}_{\mathcal{D}}^{\text{train}} = \{(V_j, Q_j, \tau_j^*)\}_{j=1}^K$ that enable evaluation of *adaptation* alongside zero-shot generalization. Let \mathcal{F}_θ be a base VLM with parameters θ , and let \mathcal{A} denote any adaptation operator (*e.g.*, PEFTs [23, 37, 25], ICL [4, 29], or TTT [18, 31]) that produces an adapted predictor g from \mathcal{F}_θ and $\mathcal{T}_{\mathcal{D}}^{\text{train}}$,

$$g = \mathcal{A}(\mathcal{F}_\theta, \mathcal{T}_{\mathcal{D}}^{\text{train}}), \quad g : (V, Q) \mapsto \hat{y}, \quad (6)$$

²Several VLMs (*e.g.*, the Gemini or Qwen series) emit bounding-box predictions only at a discrete subset of timestamps $\{t_l\}_{l=1}^L \subseteq [t_s, t_e]$ rather than at every frame.

where $\hat{y} \in \{\hat{\tau}, \{\hat{b}_t\}, [\hat{t}_s, \hat{t}_e]\}$ is the task-specific output selected by the system prompt p as in [Section 3.1](#). The benchmark is agnostic to the choice of \mathcal{A} : any method that consumes $\mathcal{T}_{\mathcal{D}}^{\text{train}}$ to produce a predictor for $\mathcal{T}_{\mathcal{D}}^{\text{test}}$ (whether by augmenting the input with retrieved demonstrations, updating a subset of θ , or full fine-tuning) is directly comparable under AnyGroundBench’s metrics.

Reference Instantiation: In-Context Learning. As a concrete reference, the main experiments instantiate \mathcal{A} as m -shot ICL, which does not require any backpropagation and is applicable to both proprietary (e.g., GPT [55], Gemini [8]) and open-source (e.g., Qwen [3, 43]) models, in which \mathcal{F}_{θ} is conditioned on m in-domain demonstrations retrieved per query (V, Q) from $\mathcal{T}_{\mathcal{D}}^{\text{train}}$ via a retrieval function \mathcal{R} ,

$$g(V, Q) = \mathcal{F}_{\theta}(V, Q | \mathcal{E}(V, Q); p), \quad \mathcal{E}(V, Q) = \mathcal{R}(V, Q; \mathcal{T}_{\mathcal{D}}^{\text{train}}, m). \quad (7)$$

The retrieval operation \mathcal{R} can be instantiated as top- m similarity retrieval based on visual similarity, textual similarity, or a combination of both.

3.3 Domain and Data Source

Animal. To advance the understanding of non-human behaviors, we include Animal Kingdom [40], capturing diverse species in natural environments. We complement this macroscopic view with a newly curated Mouse Scratching dataset, collected in a university medical department. This dataset focuses on fine-grained, high-frequency motions (e.g., distinguishing rapid scratches from continuous bouts), presenting significant challenges for precise spatio-temporal localization in clinical contexts.

Industry. Industrial workflows demand precise, multi-step human-object interactions. We use two egocentric datasets, MECCANO [44] and ENIGMA-51 [45], to capture professional activities like mechanical assembly and electrical maintenance using specialized tools.

Sports. Characterized by high-velocity, the sports domain is represented by MultiSports [34], covering disciplines like basketball and gymnastics, where fine-grained coordination is central. To elevate complexity, we introduce a novel American Football dataset capturing highly tactical, domain-specific play sequences.

Surgery. The surgical domain requires extreme precision and strict procedural adherence. We encompass two fundamental modalities: EgoSurgery [12, 13, 15] for direct manual interactions in egocentric open surgery, and CholecTrack20 [41] for instrument-mediated interventions in laparoscopic procedures. This combination covers the full spectrum of modern surgical practice, from physical manipulation to technology-assisted techniques.

Public Security. The public security domain focuses on critical incidents in public and transit environments. We utilize UCA [75] to provide an exocentric, multimodal perspective on urban surveillance, linking visual anomalies with semantic interpretations. This is complemented by DoTA [73], which addresses highly dynamic traffic accidents from an egocentric driving perspective. Together, these benchmarks span the diverse challenges of security and risk monitoring, bridging fixed urban observation and mobile accident perception.

3.4 Data Annotation

Annotators. To ensure high-quality annotations, we assembled a diverse team tailored to the specific requirements of each dataset. Annotation and data processing for the existing datasets were conducted by graduate students specializing in computer vision. For domains requiring highly specialized knowledge, we engaged domain experts. Specifically, the Mouse Scratching dataset was annotated by *two medical experts to guarantee the clinical fidelity of the captured behaviors*. The newly captured American Football dataset was annotated by *individuals with years of active playing experience*, ensuring the accurate identification and localization of complex, domain-specific actions.

Annotation Process and Quality Control. Our annotation pipeline utilizes advanced vision foundation models with rigorous human verification to ensure high-fidelity spatio-temporal grounding. The annotation process consists of the following key stages. The details are in [Appendix C](#).

1. *Textual Query and Corresponding Time Span:* For datasets equipped with existing temporal grounding annotations, we directly utilize their provided text queries. For datasets featuring other types of annotations, such as action category or anomaly localization, we manually paraphrase or annotate textual queries based on their respective labels. For the datasets without grounding

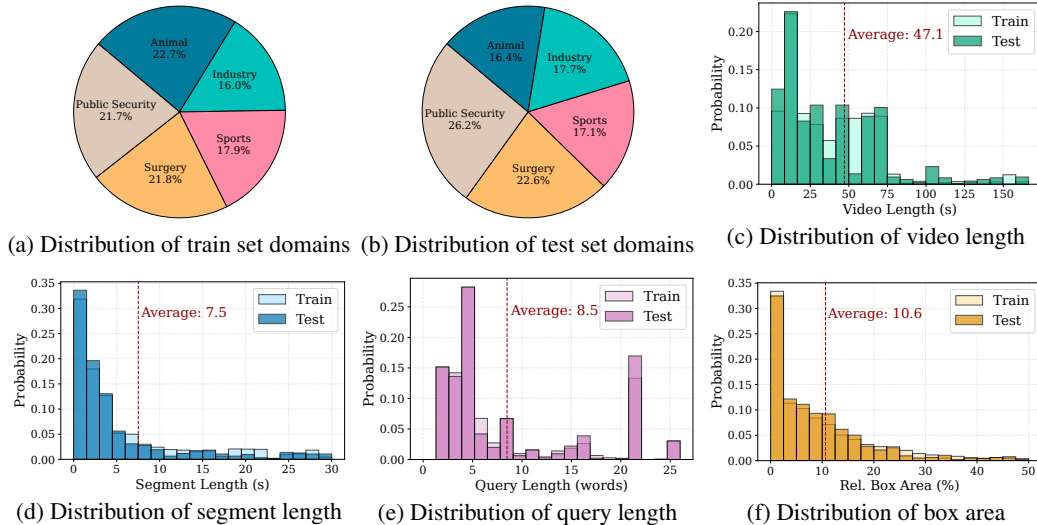


Figure 2: **Representative statistics on AnyGroundBench**, including distributions of training set domains in (a), test set domains in (b), video length (in seconds) in (c), temporal segment length (in seconds) in (d), textual query length (in words) in (e), and box area in (f).

annotations, we ask the annotators to provide the temporal time span and corresponding textual queries.

2. *Spatial Bounding Boxes*: We take a detection-then-tracking approach to label the bounding boxes within the annotated time spans in a fully automated, semi-automated, and manual manner, based on the zero-shot grounding capability of the open-vocabulary object detection (Grounding DINO [38]) and tracking (SAM2 [46]) models for each data source. The fully automated approach applies Grounding DINO to the first annotated frame with the text query input and tracks the box until the annotated end frame. In the semi-automated approach, the human annotator manually labels the corresponding box to the first frame and applies tracking. In the manual approach, the human annotators manually label the bounding box per frame. For datasets that already possess dense spatial tracking annotations, we directly adapt their existing annotations to fit our unified format.

3. *Manual Refinement*: All generated spatio-temporal boxes undergo a comprehensive manual inspection. Human annotators visually review the bounding boxes and manually correct any inaccurate bounding boxes, tracking drifts, or missing frames.

4. *Quality Control*: As a final quality control measure, refined samples are independently double-checked by at least one additional annotator, ensuring that all corrections are accurate and guarantee high reliability, annotation consistency, and fidelity in the benchmark.

3.5 Benchmark Statistics

To better understand AnyGroundBench, we display representative statistics in Figure 2. From Figure 2 (a) and (b), the 3,522 queries are evenly distributed across five specialized domains, providing a balanced testbed for domain adaptation. From Figure 2 (c) and (d), the average video length is 47.13s while the target segment is 7.51s (16% of the video length), requiring precise temporal localization within videos. Furthermore, Figure 2 (f) shows that the average relative box area is merely 10.63%, demonstrating the challenge of AnyGroundBench in grounding small, specialized visual concepts.

4 Experiments

4.1 Experimental setup

Baselines. To ensure a comprehensive evaluation, we benchmark a diverse set of VLMs, including *Proprietary models*: the GPT series (GPT-4o [1] and GPT-5.1 [55]) and the Gemini series (Gemini-2.5-

Table 2: **Main results on Spatio-Temporal (STVG), Temporal (TVG), and Spatial Video Grounding (SVG) tasks.** Each cell reports STVG / TVG / SVG, where STVG uses $vIoU@0.3$, TVG uses $tIoU@0.3$, and SVG uses $sIoU@0.3$. For each model, the first row shows the zero-shot baseline, and the second row (shaded, +ICL) shows the performance with 2-shot In-Context Learning; **purple** denotes performance improvements or ties and **red** denotes degradations relative to the zero-shot baseline.

Models	Animal	Industry	Sports	Surgery	Public Security
<i>Proprietary VLMs</i>					
GPT-4o	0.00 / 16.5 / 7.64	2.95 / 8.87 / 14.7	0.61 / 17.1 / 0.00	0.00 / 13.4 / 0.00	0.80 / 56.0 / 4.40
+ICL	0.00 / 17.3 / 12.7	1.25 / 10.4 / 4.14	0.61 / 22.0 / 0.61	0.00 / 26.1 / 0.00	6.35 / 66.9 / 6.40
GPT-5.1	3.18 / 19.7 / 55.4	5.32 / 9.46 / 28.4	0.00 / 25.7 / 1.84	1.38 / 22.6 / 0.45	4.80 / 61.2 / 35.6
+ICL	5.59 / 23.0 / 59.2	2.74 / 11.3 / 34.9	1.22 / 23.9 / 7.36	2.64 / 41.7 / 0.44	9.63 / 66.4 / 39.2
Gemini-2.5-Flash	2.54 / 26.1 / 15.2	0.59 / 21.3 / 4.73	1.84 / 31.9 / 3.68	0.00 / 22.6 / 0.97	0.40 / 51.2 / 2.00
+ICL	1.91 / 19.1 / 12.1	1.18 / 23.0 / 8.87	0.00 / 41.7 / 0.00	0.46 / 18.9 / 3.59	2.40 / 61.6 / 3.60
Gemini-2.5-Pro	8.28 / 36.9 / 20.3	1.18 / 39.6 / 17.1	0.61 / 37.4 / 7.97	1.38 / 31.4 / 2.77	4.00 / 65.8 / 22.8
+ICL	8.28 / 31.2 / 45.2	8.28 / 37.2 / 26.0	3.68 / 43.5 / 5.52	6.01 / 41.2 / 24.8	8.80 / 70.4 / 20.0
Gemini-3-Flash	14.0 / 36.3 / 51.5	5.91 / 30.7 / 20.1	2.45 / 29.4 / 2.45	0.92 / 37.9 / 11.1	10.7 / 66.8 / 45.5
+ICL	13.3 / 33.1 / 45.8	6.50 / 33.1 / 24.2	1.22 / 44.1 / 3.68	6.48 / 42.5 / 27.0	30.8 / 78.4 / 25.1
Gemini-3.1-Pro	16.5 / 37.5 / 70.7	7.69 / 21.8 / 41.4	1.22 / 26.3 / 16.5	4.16 / 32.8 / 26.1	22.8 / 69.4 / 52.0
+ICL	12.7 / 33.1 / 60.5	11.8 / 27.8 / 39.6	1.22 / 39.8 / 7.36	9.72 / 42.1 / 23.4	22.4 / 77.2 / 41.6
<i>Open-source Specialized VLMs</i>					
LLaVA-ST	12.1 / 19.7 / 53.5	0.00 / 9.46 / 12.4	0.79 / 8.58 / 3.68	0.00 / 12.0 / 0.45	0.80 / 35.6 / 13.2
<i>Open-source General-Purpose VLMs</i>					
Qwen3-VL-4B	5.73 / 25.4 / 19.7	0.00 / 4.14 / 5.32	0.00 / 8.58 / 0.00	0.00 / 13.4 / 0.00	0.40 / 39.2 / 0.00
+ICL	0.63 / 28.6 / 0.63	1.18 / 15.9 / 0.00	0.00 / 17.7 / 0.00	0.00 / 34.2 / 0.00	0.00 / 59.6 / 0.00
Qwen3-VL-8B	3.82 / 19.7 / 0.00	0.00 / 10.6 / 0.00	0.00 / 11.6 / 0.00	0.00 / 15.7 / 0.00	0.80 / 46.0 / 0.00
+ICL	0.00 / 28.0 / 4.45	0.59 / 14.7 / 0.00	0.00 / 23.3 / 0.00	0.00 / 34.2 / 0.00	0.40 / 65.6 / 0.00
Qwen3.5-4B	2.54 / 30.5 / 13.3	0.00 / 14.7 / 7.69	0.00 / 12.8 / 0.00	0.00 / 28.2 / 1.49	0.40 / 49.2 / 2.00
+ICL	3.18 / 29.2 / 17.1	2.95 / 23.6 / 5.91	0.00 / 20.8 / 0.00	0.46 / 34.7 / 6.70	2.00 / 65.2 / 2.40
Qwen3.5-9B	4.45 / 35.0 / 20.3	0.59 / 17.1 / 12.4	0.61 / 14.7 / 0.00	0.00 / 28.2 / 1.35	0.40 / 50.4 / 4.80
+ICL	2.54 / 35.0 / 10.1	1.77 / 19.5 / 14.2	0.00 / 25.7 / 0.61	0.00 / 25.4 / 7.15	2.40 / 62.8 / 2.80
Eagle2.5-8B	0.00 / 24.8 / 1.27	0.00 / 7.69 / 2.36	0.00 / 7.97 / 0.00	0.00 / 15.2 / 0.00	0.00 / 47.6 / 0.40
+ICL	0.00 / 25.4 / 0.00	0.00 / 12.4 / 0.00	0.00 / 20.8 / 0.00	0.00 / 28.2 / 0.44	0.00 / 61.6 / 0.00
InternVL3-8B	0.63 / 15.2 / 3.82	0.00 / 5.91 / 1.18	0.00 / 6.79 / 0.00	0.00 / 10.6 / 0.00	0.00 / 4.40 / 0.80
+ICL	0.00 / 15.9 / 0.00	0.00 / 7.10 / 0.00	0.00 / 7.36 / 0.00	0.00 / 25.4 / 0.00	0.00 / 7.60 / 0.00
InternVL3-14B	0.63 / 17.8 / 7.64	0.00 / 5.32 / 1.18	0.00 / 7.36 / 0.00	0.00 / 10.6 / 0.00	0.00 / 13.2 / 0.00
+ICL	0.00 / 15.2 / 0.00	0.00 / 8.59 / 0.00	0.00 / 8.64 / 0.00	0.00 / 14.5 / 0.49	0.00 / 19.0 / 0.00
InternVL3.5-8B	0.00 / 11.4 / 0.00	0.00 / 2.95 / 1.18	0.00 / 6.13 / 0.00	0.00 / 7.40 / 0.00	0.00 / 3.60 / 0.00
+ICL	0.00 / 5.09 / 1.27	0.00 / 7.81 / 2.36	0.00 / 3.68 / 0.00	0.46 / 18.0 / 2.69	0.40 / 4.00 / 0.00

Flash/Pro [8], Gemini-3-Flash [17], and Gemini-3.1-Pro), *Open-source Specialized VLMs*: LLaVA-ST [33], and *Open-source General-Purpose VLMs*: the Qwen series (Qwen3-VL-4B/8B [3] and Qwen3.5-4B/9B [43]), Eagle2.5-8B [5], and the InternVL series (InternVL3-8B/14B and InternVL3.5-8B [61]). Detailed inference configurations and full prompt templates are provided in Appendix A and Appendix B, respectively.

In-Context Learning Setup. To assess the model’s adaptability, we employ ICL as a simple baseline. Despite the simplicity, it can be universally applied to both proprietary (closed-source) and open-source models, unlike PEFTs [23, 37, 25]. Similar to [29], we utilize similarity-based selection to retrieve the $m = 2$ most relevant examples from a training pool. The retrieval is based on the weighted sum (with weight 0.5) of cosine similarity between query and candidate embeddings of textual and visual modalities, using SentenceBERT [47] and InternVideo2 [62] as the text and video encoders, respectively (Appendix A.2).

Evaluation Metrics. In accordance with established protocols [24, 33, 48, 70], we report $vIoU@0.3$ for STVG, $tIoU@0.3$ for TVG, and $sIoU@0.3$ for SVG. Results for additional threshold-based metrics, including $vIoU$, $sIoU$, and $tIoU$ at multiple thresholds, are detailed in Appendix F.

4.2 Main Results

Table 2 indicates that the STVG in specialized domains remains highly challenging for all current VLMs, including the proprietary models (e.g., Gemini-3.1-Pro). Although several models achieve

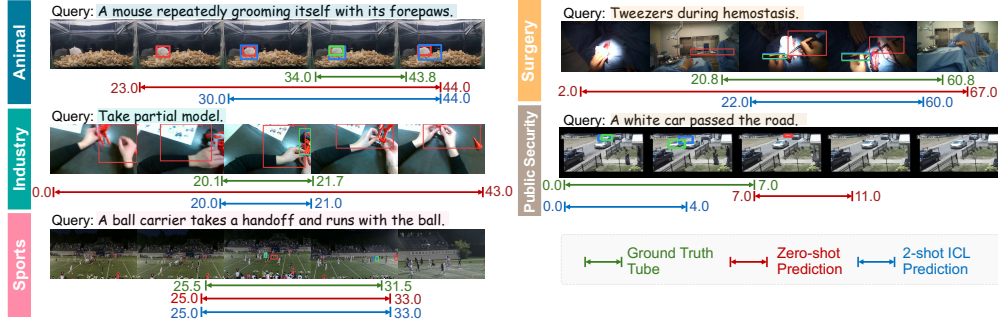


Figure 3: **Qualitative STVG results of Gemini-3.1-Pro across five specialized domains on AnyGroundBench.** Each example compares the **zero-shot prediction**, **2-shot ICL prediction**, and the **ground-truth tube** for the same query. The temporal boundaries are shown in seconds. 2-shot ICL can improve localization on some samples, but the gains are inconsistent, and spatial grounding remains fragile in specialized domains.

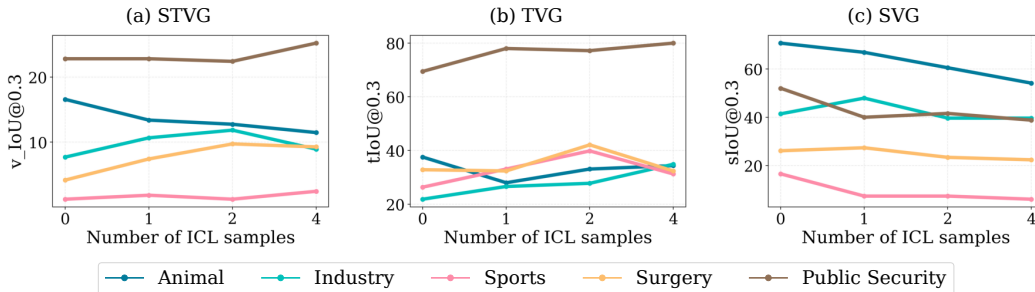


Figure 4: **Effect of the number of in-context demonstrations.** Performance on (a) STVG, (b) TVG, and (c) SVG as the number of retrieved demonstrations varies from 0 to 4. All results use Gemini-3.1-Pro.

moderate gains from ICL in specific domains (*e.g.*, 7.69 \rightarrow 11.8 with Gemini-3.1-Pro on the Industry domain), these improvements are limited and inconsistent, indicating that simple inference-time adaptation via ICL is insufficient for specialized-domain grounding. Moreover, the results with subtasks (TVG, SVG) show that TVG is often more tractable than full spatio-temporal grounding, while accurate spatial localization remains highly fragile. In summary, current VLMs still lack zero-shot grounding and adaptation capabilities to rare domains, highlighting the need for a benchmark that explicitly evaluates both domain generalization and adaptation. Detailed observation of this table is in [Appendix G](#). [Figure 3](#) presents representative visualization of Gemini-3.1-Pro’s STVG results on AnyGroundBench. The qualitative results show that both spatial and temporal grounding capabilities are improved by using the demonstrations, but are still far from accurate grounding.

4.3 Additional Analysis

Impact of the Number of Demonstrations (Figure 4). To further analyze the limited and inconsistent ICL gains in the main results, we vary the number of retrieved demonstrations from 0 to 4 for Gemini-3.1-Pro. Increasing the number of demonstrations primarily benefits TVG, whereas the average SVG score consistently drops from zero-shot to 4-shot. Meanwhile, the gains in STVG remain modest, increasing only from 10.5 (zero-shot) to 11.6 (2-shot) and 11.5 (4-shot), suggesting that simply adding more demonstrations is insufficient for adapting specialized-domain STVG.

Effectiveness of In-Context Selection Strategies (Table 3). To clarify whether the instability of ICL depends not only on the number of demonstrations but also on how examples are retrieved from the training pool, we compare the similarity calculation for the retrieval to random (no similarity is used), text-only, video-only, and text+video metrics. The best strategy is task-dependent: averaged across domains, text+video retrieval achieves the highest performance on TVG and STVG, whereas

Table 3: **Comparison of ICL sample selection strategies on STVG, TVG, and SVG.** Each cell reports STVG / TVG / SVG, where STVG uses $vIoU@0.3$, TVG uses $tIoU@0.3$, and SVG uses $sIoU@0.3$. Rows compare zero-shot and four retrieval strategies: random, text-only, video-only, and text+video retrieval.

Setting	Animal	Industry	Sports	Surgery	Public Security
zero-shot	16.6 / 37.6 / 70.7	7.69 / 21.9 / 41.4	1.23 / 26.4 / 16.6	4.17 / 32.9 / 26.1	22.8 / 69.5 / 52.0
Random	20.4 / 37.6 / 68.2	8.28 / 27.8 / 36.7	2.45 / 27.0 / 7.39	4.63 / 39.8 / 23.1	20.4 / 74.4 / 41.2
Text only	14.6 / 36.3 / 54.8	10.1 / 33.1 / 37.9	0.61 / 35.0 / 6.13	8.33 / 34.7 / 27.4	22.0 / 77.2 / 40.0
Video only	15.3 / 33.1 / 63.1	8.77 / 25.4 / 37.3	0.61 / 33.7 / 5.53	4.16 / 31.9 / 16.4	25.6 / 78.8 / 38.4
Text + Video	12.7 / 33.1 / 60.5	11.8 / 27.8 / 39.6	1.23 / 39.9 / 7.36	9.72 / 42.1 / 23.4	22.4 / 77.2 / 41.6

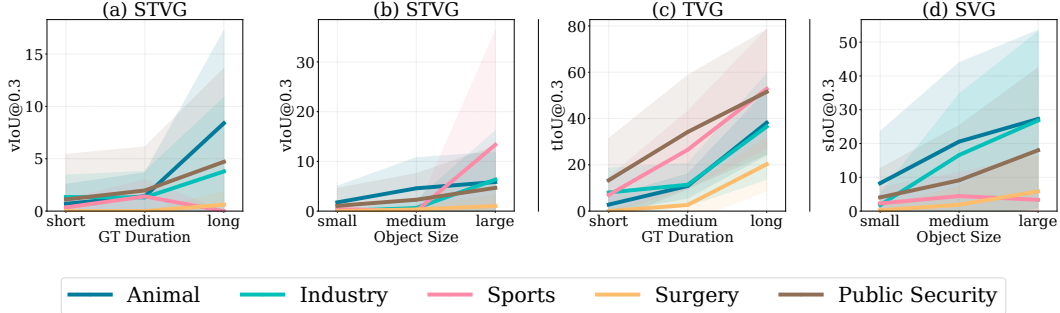


Figure 5: **Sensitivity analysis of temporal and spatial scales.** Temporal events are grouped into short (< 1 s), medium (1–3 s), and long (≥ 3 s) bins. Spatial scales are categorized by relative box area: small ($< 2.6\%$), medium (2.6%–10.0%), and large ($> 10.0\%$). All results use Gemini-3.1-Pro.

random retrieval gives the strongest SVG average. These results suggest that retrieval quality matters for ICL adaptation, but the most useful retrieval signal differs across decomposed grounding tasks.

Sensitivity to Temporal and Spatial Scales (Figure 5). We further analyze sensitivity to two fundamental sources of difficulty in STVG: ground-truth event duration and target bounding box size. For this analysis, we group sampled evaluation examples into comparable temporal-duration and object-size bins. Short events are consistently difficult to ground (a and c). Across all domains, TVG rises from 6.82 for events shorter than 1 second to 34.0 for events longer than 3 seconds, while the $vIoU$ increases more modestly from 0.74 to 3.36. This gap suggests that temporal boundary difficulty is a major source of failure for short events, but the STVG capability is constrained by spatial grounding errors.

The spatial analysis reveals a complementary pattern. Across all domains, SVG rises from 2.61 for small objects to 18.8 for large objects, while STVG rises from 0.43 to 4.43 across the same shared tertile bins. These results indicate that small or visually subtle targets are a persistent source of difficulty even when temporal ambiguity is reduced, and that this sensitivity becomes more severe in full spatio-temporal grounding.

5 Conclusion

This paper presented **AnyGroundBench**, a domain-specialized benchmark for STVG in VLMs. By spanning five specialized domains and providing both training and evaluation subsets per domain, AnyGroundBench enables evaluating the zero-shot grounding and adaptation capability of VLMs. Experiments with 15 VLMs show that specialized-domain STVG remains highly challenging: even the strongest proprietary model still lacks accurate zero-shot grounding capability, and retrieval-based ICL provides only limited and inconsistent gains. Our decomposed evaluations further reveal that TVG is often more tractable than full STVG, while spatial localization remains fragile.

Broader Impacts. AnyGroundBench provides a standardized benchmark for STVG on five specialized domains, aiming to evaluate how VLMs adapt to specialized domains such as surgery, industry, and animal behavior. By releasing AnyGroundBench with expert-annotated data with the unified format in public, we expect researchers to develop robust domain-adaptation techniques for video grounding in VLMs under a limited training data scenario.

References

- [1] Josh Achiam, Steven Adler, Sandhini Agarwal, Lama Ahmad, Ilge Akkaya, Florencia Leoni Aleman, Diogo Almeida, Janko Altschmidt, Sam Altman, Shyamal Anadkat, et al. Gpt-4 Technical Report. *arXiv preprint arXiv:2303.08774*, 2023.
- [2] Ghazi Shazan Ahmad, Ahmed Heakl, Hanan Gani, Abdelrahman Shaker, Zhiqiang Shen, Fahad Shahbaz Khan, and Salman Khan. VideoMolmo: Spatio-Temporal Grounding Meets Pointing. *arXiv preprint arXiv:2506.05336*, 2025.
- [3] Shuai Bai, Yuxuan Cai, Ruizhe Chen, Keqin Chen, Xionghui Chen, Zesen Cheng, Lianghao Deng, Wei Ding, Chang Gao, Chunjiang Ge, Wenbin Ge, Zhifang Guo, Qidong Huang, Jie Huang, Fei Huang, Binyuan Hui, Shutong Jiang, Zhaohai Li, Mingsheng Li, Mei Li, Kaixin Li, Zicheng Lin, Junyang Lin, Xuejing Liu, Jiawei Liu, Chenglong Liu, Yang Liu, Dayiheng Liu, Shixuan Liu, Dunjie Lu, Ruilin Luo, Chenxu Lv, Rui Men, Lingchen Meng, Xuancheng Ren, Xingzhang Ren, Sibao Song, Yuchong Sun, Jun Tang, Jianhong Tu, Jianqiang Wan, Peng Wang, Pengfei Wang, Qiuyue Wang, Yuxuan Wang, Tianbao Xie, Yiheng Xu, Haiyang Xu, Jin Xu, Zhibo Yang, Mingkun Yang, Jianxin Yang, An Yang, Bowen Yu, Fei Zhang, Hang Zhang, Xi Zhang, Bo Zheng, Humen Zhong, Jingren Zhou, Fan Zhou, Jing Zhou, Yuanzhi Zhu, and Ke Zhu. Qwen3-VL Technical Report. *arXiv preprint arXiv:2511.21631*, 2025.
- [4] Tom Brown, Benjamin Mann, Nick Ryder, Melanie Subbiah, Jared D Kaplan, Prafulla Dhariwal, Arvind Neelakantan, Pranav Shyam, Girish Sastry, Amanda Askell, et al. Language Models are Few-Shot Learners. In *NeurIPS*, 2020.
- [5] Guo Chen, Zhiqi Li, Shihao Wang, Jindong Jiang, Yicheng Liu, Lidong Lu, De-An Huang, Wonmin Byeon, Matthieu Le, Max Ehrlich, Tong Lu, Limin Wang, Bryan Catanzaro, Jan Kautz, Andrew Tao, Zhiding Yu, and Guilin Liu. Eagle 2.5: Boosting Long-Context Post-Training for Frontier Vision-Language Models. In *NeurIPS*, 2026.
- [6] Zhenfang Chen, Lin Ma, Wenhan Luo, and Kwan-Yee Kenneth Wong. Weakly-Supervised Spatio-Temporally Grounding Natural Sentence in Video. In *ACL*, 2019.
- [7] Zixu Cheng, Jian Hu, Ziquan Liu, Chenyang Si, Wei Li, and Shaogang Gong. V-STaR: Benchmarking Video-LLMs on Video Spatio-Temporal Reasoning. *arXiv preprint arXiv:2503.11495*, 2025.
- [8] Gheorghe Comanici, Eric Bieber, Mike Schaekermann, Ice Pasupat, Noveen Sachdeva, Inderjit Dhillon, Marcel Blistein, Ori Ram, Dan Zhang, Evan Rosen, et al. Gemini 2.5: Pushing the Frontier with Advanced Reasoning, Multimodality, Long Context, and Next Generation Agentic Capabilities. *arXiv preprint arXiv:2507.06261*, 2025.
- [9] Henghui Ding, Chang Liu, Shuting He, Xudong Jiang, and Chen Change Loy. MeViS: A Large-scale Benchmark for Video Segmentation with Motion Expressions. In *ICCV*, 2023.
- [10] Yuhao Dong, Shulin Tian, Shuai Liu, Shuangrui Ding, Yuhang Zang, Xiaoyi Dong, Yuhang Cao, Jiaqi Wang, and Ziwei Liu. Demo-ICL: In-Context Learning for Procedural Video Knowledge Acquisition. *arXiv preprint arXiv:2602.08439*, 2026.
- [11] Chaoyou Fu, Yuhan Dai, Yongdong Luo, Lei Li, Shuhuai Ren, Renrui Zhang, Zihan Wang, Chenyu Zhou, Yunhang Shen, Mengdan Zhang, Peixian Chen, Yanwei Li, Shaohui Lin, Sirui Zhao, Ke Li, Tong Xu, Xiawu Zheng, Enhong Chen, Caifeng Shan, Ran He, and Xing Sun. Video-MME: The First-Ever Comprehensive Evaluation Benchmark of Multi-modal LLMs in Video Analysis. In *CVPR*, 2025.
- [12] Ryo Fujii, Ryo Hachiuma, Hiroki Kajita, and Hideo Saito. Surgical Tool Detection in Open Surgery Videos. *Applied Sciences*, 2022.
- [13] Ryo Fujii, Masashi Hatano, Hideo Saito, and Hiroki Kajita. EgoSurgery-Phase: A Dataset of Surgical Phase Recognition from Egocentric Open Surgery Videos. In *MICCAI*, 2024.
- [14] Ryo Fujii, Hideo Saito, and Ryo Hachiuma. VIOLA: Towards Video In-Context Learning with Minimal Annotations. *arXiv preprint arXiv:2601.15549*, 2026.
- [15] Ryo Fujii, Hideo Saito, and Hiroki Kajita. EgoSurgery-Tool: A Dataset of Surgical Tool and Hand Detection from Egocentric Open Surgery Videos. *arXiv preprint arXiv:2406.03095*, 2024.
- [16] Hong Gao, Jingyu Wu, Xiangkai Xu, Kangni Xie, Yunchen Zhang, Bin Zhong, Xurui Gao, and Min-Ling Zhang. OmniGround: A Comprehensive Spatio-Temporal Grounding Benchmark for Real-World Complex Scenarios. In *CVPR*, 2026.

- [17] Google DeepMind. Gemini 3 Flash Model Card. <https://storage.googleapis.com/deepmind-media/Model-Cards/Gemini-3-Flash-Model-Card.pdf>, 2025.
- [18] Halil Alperen Gozeten, M. Emrullah Ildiz, Xuechen Zhang, Mahdi Soltanolkotabi, Marco Mondelli, and Samet Oymak. Test-Time Training Provably Improves Transformers as In-context Learners. In *ICML*, 2025.
- [19] Chunhui Gu, Chen Sun, David A. Ross, Carl Vondrick, Caroline Pantofaru, Yeqing Li, Sudheendra Vijayanarasimhan, George Toderici, Susanna Ricco, Rahul Sukthankar, Cordelia Schmid, and Jitendra Malik. AVA: A Video Dataset of Spatio-Temporally Localized Atomic Visual Actions. In *CVPR*, 2018.
- [20] Xin Gu, Heng Fan, Yan Huang, Tiejian Luo, and Libo Zhang. Context-Guided Spatio-Temporal Video Grounding. In *CVPR*, 2024.
- [21] Xin Gu, Haoji Zhang, Qihang Fan, Jingxuan Niu, Zhipeng Zhang, Libo Zhang, Guang Chen, Fan Chen, Longyin Wen, and Sijie Zhu. Thinking With Bounding Boxes: Enhancing Spatio-Temporal Video Grounding via Reinforcement Fine-Tuning. *arXiv preprint arXiv:2511.21375*, 2025.
- [22] Miran Heo, Min-Hung Chen, De-An Huang, Sifei Liu, Subhashree Radhakrishnan, Seon Joo Kim, Yu-Chiang Frank Wang, and Ryo Hachiuma. Omni-RGPT: Unifying Image and Video Region-level Understanding via Token Marks. In *CVPR*, 2025.
- [23] Edward J Hu, yelong shen, Phillip Wallis, Zeyuan Allen-Zhu, Yuanzhi Li, Shean Wang, Lu Wang, and Weizhu Chen. LoRA: Low-Rank Adaptation of Large Language Models. In *ICLR*, 2022.
- [24] Bin Huang, Xin Wang, Hong Chen, Zihan Song, and Wenwu Zhu. VTimeLLM: Empower LLM to Grasp Video Moments. In *CVPR*, 2024.
- [25] Menglin Jia, Luming Tang, Bor-Chun Chen, Claire Cardie, Serge Belongie, Bharath Hariharan, and Ser-Nam Lim. Visual Prompt Tuning. In *ECCV*, 2022.
- [26] Yang Jin, yongzhi li, Zehuan Yuan, and Yadong MU. Embracing Consistency: A One-Stage Approach for Spatio-Temporal Video Grounding. In *NeurIPS*, 2022.
- [27] Allan V Kalueff, Adam Michael Stewart, Cai Song, Kent C Berridge, Ann M Graybiel, and John C Fentress. Neurobiology of Rodent Self-Grooming and Its Value for Translational Neuroscience. *Nature Reviews Neuroscience*, 2016.
- [28] Dahye Kim, Jungin Park, Jiyoung Lee, Seongheon Park, and Kwanghoon Sohn. Language-Free Training for Zero-Shot Video Grounding. In *WACV*, 2023.
- [29] Kangsan Kim, Geon Park, Youngwan Lee, Woongyeong Yeo, and Sung Ju Hwang. VideoICL: Confidence-based Iterative In-context Learning for Out-of-Distribution Video Understanding. In *CVPR*, 2025.
- [30] Shuhei Kurita, Naoki Katsura, and Eri Onami. RefEgo: Referring Expression Comprehension Dataset from First-Person Perception of Ego4D. In *ICCV*, 2023.
- [31] Kento Kuwataka and Taiji Suzuki. Test-Time Training Enhances In-Context Learning of Nonlinear Functions. *arXiv preprint 2509.25741*, 2026.
- [32] Chenglin Li, Qianglong Chen, Feng Han, Yikun Wang, Xingxi Yin, Yan Gong, Ruilin Li, Yin Zhang, and Jiaqi Wang. VideoThinker: Building Agentic VideoLLMs with LLM-Guided Tool Reasoning. *arXiv preprint 2601.15724*, 2026.
- [33] Hongyu Li, Jinyu Chen, Ziyu Wei, Shaofei Huang, Tianrui Hui, Jialin Gao, Xiaoming Wei, and Si Liu. LLaVA-ST: A Multimodal Large Language Model for Fine-Grained Spatial-Temporal Understanding. In *CVPR*, 2025.
- [34] Yixuan Li, Lei Chen, Runyu He, Zhenzhi Wang, Gangshan Wu, and Limin Wang. MultiSports: A Multi-Person Video Dataset of Spatio-Temporally Localized Sports Actions. In *ICCV*, 2021.
- [35] Zhaowei Li, Qi Xu, Dong Zhang, Hang Song, YiQing Cai, Qi Qi, Ran Zhou, Juntong Pan, Zefeng Li, Yu Tu, Zhida Huang, and Tao Wang. GroundingGPT: Language Enhanced Multi-modal Grounding Model. In *ACL*, 2024.
- [36] Shuo Liang, Yiwu Zhong, Zi-Yuan Hu, Yeyao Tao, and Liwei Wang. Fine-grained Spatiotemporal Grounding on Egocentric Videos. In *ICCV*, 2025.
- [37] Shih-Yang Liu, Chien-Yi Wang, Hongxu Yin, Pavlo Molchanov, Yu-Chiang Frank Wang, Kwang-Ting Cheng, and Min-Hung Chen. DoRA: Weight-Decomposed Low-Rank Adaptation. In *ICML*, 2024.

- [38] Shilong Liu, Zhaoyang Zeng, Tianhe Ren, Feng Li, Hao Zhang, Jie Yang, Qing Jiang, Chunyuan Li, Jianwei Yang, Hang Su, Jun Zhu, and Lei Zhang. Grounding DINO: Marrying DINO with Grounded Pre-Training for Open-Set Object Detection. In *ECCV*, 2024.
- [39] Jiahao Meng, Xiangtai Li, Haochen Wang, Yue Tan, Tao Zhang, Lingdong Kong, Yunhai Tong, Anran Wang, Zhiyang Teng, Yujing Wang, and Zhuochen Wang. Open-o3 Video: Grounded Video Reasoning with Explicit Spatio-Temporal Evidence. *arXiv preprint arXiv:2510.20579*, 2025.
- [40] Xun Long Ng, Kian Eng Ong, Qichen Zheng, Yun Ni, Si Yong Yeo, and Jun Liu. Animal Kingdom: A Large and Diverse Dataset for Animal Behavior Understanding. In *CVPR*, 2022.
- [41] Chinedu Innocent Nwoye, Kareem Elgohary, Anvita Srinivas, Fauzan Zaid, Joël L. Lavanchy, and Nicolas Padoy. CholecTrack20: A Multi-Perspective Tracking Dataset for Surgical Tools. In *CVPR*, 2025.
- [42] Pramanick, Shraman and Mavroudi, Effrosyni and Song, Yale and Chellappa, Rama and Torresani, Lorenzo and Afouras, Triantafyllos. Enrich and Detect: Video Temporal Grounding with Multimodal LLMs. In *ICCV*, 2025.
- [43] Qwen Team. Qwen3.5: Towards Native Multimodal Agents, February 2026.
- [44] Francesco Ragusa, Antonino Furnari, and Giovanni Maria Farinella. MECCANO: A Multimodal Egocentric Dataset for Humans Behavior Understanding in the Industrial-like Domain . *CVIM*, 2023.
- [45] Francesco Ragusa, Rosario Leonardi, Michele Mazzamuto, Claudia Bonanno, Rosario Scavo, Antonino Furnari, and Giovanni Maria Farinella. ENIGMA-51: Towards a Fine-Grained Understanding of Human Behavior in Industrial Scenarios. In *WACV*, 2024.
- [46] Nikhila Ravi, Valentin Gabeur, Yuan-Ting Hu, Ronghang Hu, Chaitanya Ryali, Tengyu Ma, Haitham Khedr, Roman Rädle, Chloe Rolland, Laura Gustafson, Eric Mintun, Junting Pan, Kalyan Vasudev Alwala, Nicolas Carion, Chao-Yuan Wu, Ross Girshick, Piotr Dollar, and Christoph Feichtenhofer. SAM 2: Segment Anything in Images and Videos. In *ICLR*, 2025.
- [47] Nils Reimers and Iryna Gurevych. Sentence-BERT: Sentence Embeddings using Siamese BERT-Networks. In *EMNLP-IJCNLP*, 2019.
- [48] Shuhuai Ren, Linli Yao, Shicheng Li, Xu Sun, and Lu Hou. TimeChat: A Time-sensitive Multimodal Large Language Model for Long Video Understanding. In *CVPR*, 2024.
- [49] Ohad Rubin, Jonathan Herzig, and Jonathan Berant. Learning To Retrieve Prompts for In-Context Learning. In *NAACL*, 2022.
- [50] Cristina Segalin, Jalani Williams, Tomomi Karigo, May Hui, Moriel Zelikowsky, Jennifer J Sun, Pietro Perona, David J Anderson, and Ann Kennedy. The Mouse Action Recognition System (MARS) software pipeline for automated analysis of social behaviors in mice. *eLife*, 2021.
- [51] Seonguk Seo, Joon-Young Lee, and Bohyung Han. URVOS: Unified Referring Video Object Segmentation Network with a Large-Scale Benchmark. In *ECCV*, 2020.
- [52] Xindi Shang, Donglin Di, Junbin Xiao, Yu Cao, Xun Yang, and Tat-Seng Chua. Annotating Objects and Relations in User-Generated Videos. In *ICMR*, 2019.
- [53] Xiaoqian Shen, Min-Hung Chen, Yu-Chiang Frank Wang, Mohamed Elhoseiny, and Ryo Hachiuma. Zoom-Zero: Reinforced Coarse-to-Fine Video Understanding via Temporal Zoom-in. *arXiv preprint arXiv:2512.14273*, 2025.
- [54] Jiapeng Shi, Junke Wang, Zuyao You, Bo He, and Zuxuan Wu. VideoLoom: A Video Large Language Model for Joint Spatial-Temporal Understanding. In *ICML*, 2026.
- [55] Aaditya Singh, Adam Fry, Adam Perelman, Adam Tart, Adi Ganesh, Ahmed El-Kishky, Aidan McLaughlin, Aiden Low, AJ Ostrow, Akhila Ananthram, et al. OpenAI GPT-5 System Card. *arXiv preprint arXiv:2601.03267*, 2025.
- [56] Rui Su, Qian Yu, and Dong Xu. STVGBert: A Visual-Linguistic Transformer Based Framework for Spatio-Temporal Video Grounding. In *ICCV*, 2021.
- [57] Waqas Sultani, Chen Chen, and Mubarak Shah. Real-World Anomaly Detection in Surveillance Videos. In *CVPR*, 2018.
- [58] Zongheng Tang, Yue Liao, Si Liu, Guanbin Li, Xiaojie Jin, Hongxu Jiang, Qian Yu, and Dong Xu. Human-Centric Spatio-Temporal Video Grounding With Visual Transformers. *TCSVT*, 2022.

- [59] Vidi Team, Chia-Wen Kuo, Chuang Huang, Dawei Du, Fan Chen, Fanding Lei, Feng Gao, Guang Chen, Haoji Zhang, Haojun Zhao, Jin Liu, Jingjing Zhuge, Lili Fang, Lingxi Zhang, Longyin Wen, Lu Guo, Lu Xu, Lusha Li, Qihang Fan, Rachel Deng, Shaobo Fang, Shu Zhang, Sijie Zhu, Stuart Siew, Weiyao Tao, Wen Zhong, Xiaohui Shen, Xin Gu, Ye Yuan, Yicheng He, Yiming Cui, Zhenfang Chen, Zhihua Wu, and Zuhua Lin. Vidi2.5: Large Multimodal Models for Video Understanding and Creation. *arXiv preprint arXiv:2511.19529*, 2026.
- [60] Jiankang Wang, Zhihan Zhang, Zhihang Liu, Yang Li, Jiannan Ge, Hongtao Xie, and Yongdong Zhang. SpaceVLLM: Endowing Multimodal Large Language Model with Spatio-Temporal Video Grounding Capability. In *AAAI*, 2026.
- [61] Weiyun Wang, Zhangwei Gao, Lixin Gu, Hengjun Pu, Long Cui, Xingguang Wei, Zhaoyang Liu, Linglin Jing, Shenglong Ye, Jie Shao, et al. InternVL3.5: Advancing Open-Source Multimodal Models in Versatility, Reasoning, and Efficiency. *arXiv preprint arXiv:2508.18265*, 2025.
- [62] Yi Wang, Kunchang Li, Xinhao Li, Jiashuo Yu, Yinan He, Guo Chen, Baoqi Pei, Rongkun Zheng, Zun Wang, Yansong Shi, et al. InternVideo2: Scaling Foundation Models for Multimodal Video Understanding. In *ECCV*, 2024.
- [63] Syed Talal Wasim, Muzammal Naseer, Salman Khan, Ming-Hsuan Yang, and Fahad Shahbaz Khan. VideoGrounding-DINO: Towards Open-Vocabulary Spatio-Temporal Video Grounding. In *CVPR*, 2024.
- [64] Junbin Xiao, Angela Yao, Yicong Li, and Tat-Seng Chua. Can I Trust Your Answer? Visually Grounded Video Question Answering. In *CVPR*, 2024.
- [65] Sang Michael Xie, Aditi Raghunathan, Percy Liang, and Tengyu Ma. An Explanation of In-context Learning as Implicit Bayesian Inference. In *ICLR*, 2022.
- [66] Qi'ao Xu, Tianwen Qian, Yuqian Fu, Kailing Li, Yang Jiao, Jiacheng Zhang, Xiaoling Wang, and Liang He. ToG-Bench: Task-Oriented Spatio-Temporal Grounding in Egocentric Videos. *arXiv preprint arXiv:2512.03666*, 2025.
- [67] Zihui Xue, Ami Baid, Sangho Kim, Mi Luo, and Kristen Grauman. Personal Visual Context Learning in Large Multimodal Models. *arXiv preprint arXiv:2605.10936*, 2026.
- [68] Masataka Yamaguchi, Kuniaki Saito, Yoshitaka Ushiku, and Tatsuya Harada. Spatio-Temporal Person Retrieval via Natural Language Queries. In *ICCV*, 2017.
- [69] Ziang Yan, Xinhao Li, Yinan He, Zhengrong Yue, Xiangyu Zeng, Yali Wang, Yu Qiao, Limin Wang, and Yi Wang. VideoChat-R1.5: Visual Test-Time Scaling to Reinforce Multimodal Reasoning by Iterative Perception. *arXiv preprint arXiv:2509.21100*, 2025.
- [70] Antoine Yang, Antoine Miech, Josef Sivic, Ivan Laptev, and Cordelia Schmid. TubeDETR: Spatio-Temporal Video Grounding with Transformers. In *CVPR*, 2022.
- [71] Zaiquan Yang, Yuhao LIU, Gerhard Petrus Hancke, and Rynson W. H. Lau. Unleashing the Potential of Multimodal LLMs for Zero-Shot Spatio-Temporal Video Grounding. In *NeurIPS*, 2025.
- [72] Jiali Yao, Xin Gu, Xinran Deng, Mengrui Dai, Bing Fan, Zhipeng Zhang, Yan Huang, Heng Fan, and Libo Zhang. OmniSTVG: Toward Spatio-Temporal Omni-Object Video Grounding. In *ICLR*, 2026.
- [73] Yu Yao, Xizi Wang, Mingze Xu, Zelin Pu, Yuchen Wang, Ella Atkins, and David J. Crandall. DoTA: Unsupervised Detection of Traffic Anomaly in Driving Videos. *TPAMI*, 2023.
- [74] Keunwoo Peter Yu, Zheyuan Zhang, Fengyuan Hu, Shane Storks, and Joyce Chai. Eliciting In-Context Learning in Vision-Language Models for Videos Through Curated Data Distributional Properties. In *EMNLP*, 2024.
- [75] Tongtong Yuan, Xuange Zhang, Kun Liu, Bo Liu, Chen Chen, Jian Jin, and Zhenzhen Jiao. Towards Surveillance Video-and-Language Understanding: New Dataset, Baselines, and Challenges. In *CVPR*, 2024.
- [76] Shuang Zeng, Xinyuan Chang, Mengwei Xie, Xinran Liu, Yifan Bai, Zheng Pan, Mu Xu, and Xing Wei. FutureSightDrive: Thinking Visually with Spatio-Temporal CoT for Autonomous Driving. In *NeurIPS*, 2025.
- [77] Xiaowen Zhang, Zhi Gao, Licheng Jiao, Lingling Li, and Qing Li. STVG-R1: Incentivizing Instance-Level Reasoning and Grounding in Videos via Reinforcement Learning. In *ICLR*, 2026.

- [78] Zhu Zhang, Zhou Zhao, Yang Zhao, Qi Wang, Huasheng Liu, and Lianli Gao. Where Does It Exist: Spatio-Temporal Video Grounding for Multi-Form Sentences. In *CVPR*, 2020.
- [79] Junjie Zhou, Yan Shu, Bo Zhao, Boya Wu, Zhengyang Liang, Shitao Xiao, Minghao Qin, Xi Yang, Yongping Xiong, Bo Zhang, Tiejun Huang, and Zheng Liu. MLVU: Benchmarking Multi-task Long Video Understanding. In *CVPR*, 2025.
- [80] Jinguo Zhu, Weiyun Wang, Zhe Chen, Zhaoyang Liu, Shenglong Ye, Lixin Gu, Hao Tian, Yuchen Duan, Weijie Su, Jie Shao, et al. InternVL3: Exploring Advanced Training and Test-Time Recipes for Open-Source Multimodal Models. *arXiv preprint arXiv:2504.10479*, 2025.

Appendix

A Implementation and Inference Details

A.1 Inference Configuration

Model-Specific Parameters. Unless otherwise noted, we employed the default inference configurations for each model or API. Specific exceptions were made for the following models: for Qwen3.5 [43], we disabled “thinking mode” because preliminary trials with five retries on a dataset showed that most output tokens were spent on free-form reasoning text, preventing the models from reliably following the required timestamp and bounding-box output format; for Eagle 2.5 [5], five preliminary experiments with the default setting failed to follow the required output format, and therefore we used `do_sample=True`, `top_p=0.95`, a temperature of 0.8, and a maximum of 1024 new tokens to allow natural generation while improving instruction following; and for LLaVA-ST [33], we used `do_sample=True`, a temperature of 0.01, and 1 beam. For all other models, output-length limits were set to 64 tokens for temporal grounding and 4096 tokens for spatial and spatio-temporal grounding.

Video Preprocessing. The default preprocessing involved an explicit sampling rate of 1 fps with a maximum of 120 frames, which was applied to Qwen3-VL [3], Qwen3.5, Eagle 2.5, InternVL-3 [80] and InternVL-3.5 [61]. For GPT models [1, 55], videos up to 120 seconds were sampled at 1 fps, while longer videos were capped at 120 frames. All sampled frames were resized to a maximum resolution of 512 pixels on the longer side. For LLaVA-ST, query videos were processed with a fixed budget of 100 sampled frames. These preprocessing configurations were consistently applied to both query and in-context videos. For InternVL-3/3.5, the sampled frame counts of demonstration videos were dynamically adjusted to match those of the query video during the in-context learning process.

A.2 In-Context Learning Setup

For our few-shot evaluations, we provide $m = 2$ demonstrations retrieved from the domain-specific training split. Following [29], we calculate a hybrid retrieval score S to select the most relevant examples for each query. This score is defined as the weighted sum of visual and textual cosine similarities:

$$S = (1 - \alpha)s_{\text{visual}} + \alpha s_{\text{text}} \quad (8)$$

where s_{visual} and s_{text} denote the cosine similarities calculated using InternVideo2 [62] and SentenceBERT [47] embeddings, respectively. We set the weighting coefficient $\alpha = 0.5$ across all experiments to balance the influence of both modalities.

A.3 Computational Requirements

All local open-source model experiments were conducted on two internal GPU servers. One internal GPU server was equipped with NVIDIA RTX 5090 (32GB) and NVIDIA RTX PRO 5000 Blackwell (48GB) GPUs. Another internal GPU server was equipped with NVIDIA A100 (80GB) GPUs. API-based experiments with GPT and Gemini models were conducted through their official APIs.

B Prompts

To ensure reproducibility and foster future spatio-temporal grounding research, we provide the prompts used to evaluate open-source models (Qwen3-VL [3], Qwen3.5 [43], InternVL-3 [80], InternVL-3.5 [61], and Eagle 2.5 [5]), proprietary models (Gemini-2.5-Flash/Pro [8], Gemini-3-Flash [17], Gemini-3.1-Pro, GPT-4o [1] and GPT-5.1 [55]), and the specialist LLaVA-ST model [33].

The requested response format differs across model families in temporal identifiers, bounding-box coordinate order, and coordinate scale. For Gemini and GPT models, we followed their official API documentation.³ For Qwen3-VL, InternVL-3, InternVL-3.5, and LLaVA-ST, we followed their

³Gemini: <https://ai.google.dev/gemini-api/docs/image-understanding> and <https://ai.google.dev/gemini-api/docs/video-understanding>; OpenAI: <https://platform.openai.com/docs/guides/vision>.

Table 4: Model-specific response formats requested during inference. The raw model outputs are parsed and normalized during evaluation, but the requested surface format differs by model family along three axes: temporal identifier, box order, and coordinate scale.

Model family	Temporal identifier	Box order	Coordinate scale
Gemini	Timestamp (MM:SS)	[yxyx]	0–1000 normalized
GPT	Frame index	[xyxy]	0–1 normalized
General open-source MLLMs	Timestamp in seconds	[xyxy]	0–1000 normalized
LLaVA-ST	Temporal token	[xyxy]	temporal and spatial tokens in 0–99

technical reports, documentation, or released code [3, 80, 61, 33].⁴ For Qwen3.5 and Eagle 2.5, we did not find a model-specific grounding-output schema in the released paper or code [5], so we used the same open-source prompt format selected by preliminary parsing trials; see Section A.1. Table 4 summarizes the detailed response format used for each model family; all outputs are subsequently parsed and converted into a unified internal representation before evaluation.

The full prompt text for each task and model family is listed below.

B.1 Temporal Grounding

We use model-family-specific temporal grounding prompts.

Gemini family (adapted from Vidi2.5 [59]).

Prompt Template: Gemini Family (Temporal)

Answer with time ranges and do not output explanation.
 What is the single time range corresponding to the text query: {query}?
 Output format: [start, end]

GPT family (adapted from Vidi2.5 [59]).

Prompt Template: GPT Family (Temporal)

The input images are frames from a video.
 Output the frame indexes that correspond to the text query: {query}.
 Only output the index range (e.g., 2-4, 6-8).

General open-source MLLMs (adapted from Qwen3-VL [3]). We use this template for Qwen3-VL, Qwen3.5, InternVL3, InternVL3.5, and Eagle 2.5.

Prompt Template: General Open-Source MLLMs (Temporal)

Give you a textual query: {query}
 When does the described content occur in the video?
 Please return the timestamp in seconds.
 Output format: [start, end].

LLaVA-ST [33].

Prompt Template: LLaVA-ST (Temporal)

Give you a textual query: {query}
 When does the described content occur in the video?
 Please return the start and end timestamps.

⁴InternVL documentation: https://internvl.readthedocs.io/en/latest/get_started/chat_data_format.html; LLaVA-ST code: <https://github.com/appletea233/LLaVA-ST>.

B.2 Spatial Grounding

We use model-family-specific spatial grounding prompts.

Gemini family.

Prompt Template: Gemini Family (Spatial)

Answer with bounding boxes and do not output explanation.
Bounding box format: [y_min, x_min, y_max, x_max] with values in [0, 1000] normalized to the video frame.
What are all the positions corresponding to the text query: {query}?
Output format: ["timestamp": "00:30", "bbox_2d": [100, 200, 300, 400], ...]

GPT family.

Prompt Template: GPT Family (Spatial)

Given the frames of video, please find all the objects corresponding to the text query: "{query}"
Output only a JSON array.
Frame index format: 0-based integer.
Bounding box format: [x_min, y_min, x_max, y_max] with normalized value in 0.000 – 1.000.
Example: ["frame_id": 1, "bbox_2d": [x_min, y_min, x_max, y_max], ...]

General open-source MLLMs.

Prompt Template: General Open-Source MLLMs (Spatial)

Given the query "{query}", for each frame, detect and localize the visual content described by the textual query.
If the visual content does not exist in a frame, skip that frame.
Output the results in JSON format.
Example: ["timestamp": 1.0, "bbox_2d": [x_min, y_min, x_max, y_max], ...]

LLaVA-ST [33].

Prompt Template: LLaVA-ST (Spatial)

Between {<TEMP-000><TEMP-099>}, "{query}".
Please describe the location of the corresponding subject/object in this video.
Please give the spatial bounding box corresponding to each timestamp in the time period.

B.3 Spatio-Temporal Grounding

We use model-family-specific spatio-temporal grounding prompts.

Gemini family (adapted from Vidi2.5 [59]).

Prompt Template: Gemini Family (Spatio-Temporal)

Answer with timestamps and bounding boxes and do not output explanation.
Output only a JSON array.
Timestamp format: MM:SS with zero-padding (00–59 for MM and SS).
Bounding box format: [y_min, x_min, y_max, x_max] with values in [0, 1000] normalized to the video frame.
Example: [{"timestamp": "00:30", "box_2d": [100, 200, 300, 400], ...}]
What are all the timestamps and positions corresponding to the text query: "{query}"?

GPT family (adapted from Vidi2.5 [59]).

Prompt Template: GPT Family (Spatio-Temporal)

Given the frames of video, please find all the objects corresponding to the text query: "{query}"
Output only a JSON array.
Frame index format: 0-based integer.
Bounding box format: [x_min, y_min, x_max, y_max] (0.000 – 1.000 normalized).
Example: [{"frame": 3, "box": [0.051, 0.252, 0.323, 0.954], ...}]

General open-source MLLMs (adapted from Qwen3-VL [3]).

Prompt Template: General Open-Source MLLMs (Spatio-Temporal)

Given the query "{query}", for each frame, detect and localize the visual content described by the textual query.
If the visual content does not exist in a frame, skip that frame.
Output the results in JSON format.
Example: [{"timestamp": 1.0, "bbox_2d": [x_min, y_min, x_max, y_max], ...}]

LLaVA-ST [33].

Prompt Template: LLaVA-ST (Spatio-Temporal)

When does "{query}" occur in the video?
Please describe the location of the corresponding subject/object in this video.
Please firstly give the timestamps, and then give the spatial bounding box corresponding to each timestamp in the time period.

C Details of Constituent Datasets

AnyGroundBench consists of ten datasets spanning five specialized domains: animal, industry, sports, surgery, and public security. The specific characteristics, curation processes, and annotation enhancements for each constituent dataset are detailed below.

Animal Kingdom [40]. Animal Kingdom is a large-scale dataset featuring 850 species across 50 hours of video. While it provides multiple annotation types, including action recognition and pose estimation, we specifically utilize the temporal grounding subset. We extended the original temporal boundaries by annotating per-frame spatial bounding boxes for the target animals. This converts the original temporal-only labels into a Spatio-Temporal Video Grounding (STVG) format, focusing on diverse behaviors in complex natural environments.

Mouse Scratching. Mouse Scratching is a specialized, clinical-grade spatio-temporal grounding benchmark newly curated by two board-certified plastic surgeons to evaluate therapeutic efficacy in atopic dermatitis mouse models, with additional relevance to neurology and psychiatry for detecting nuanced behaviors like facial scratching. Figure 6 provides additional qualitative examples from the

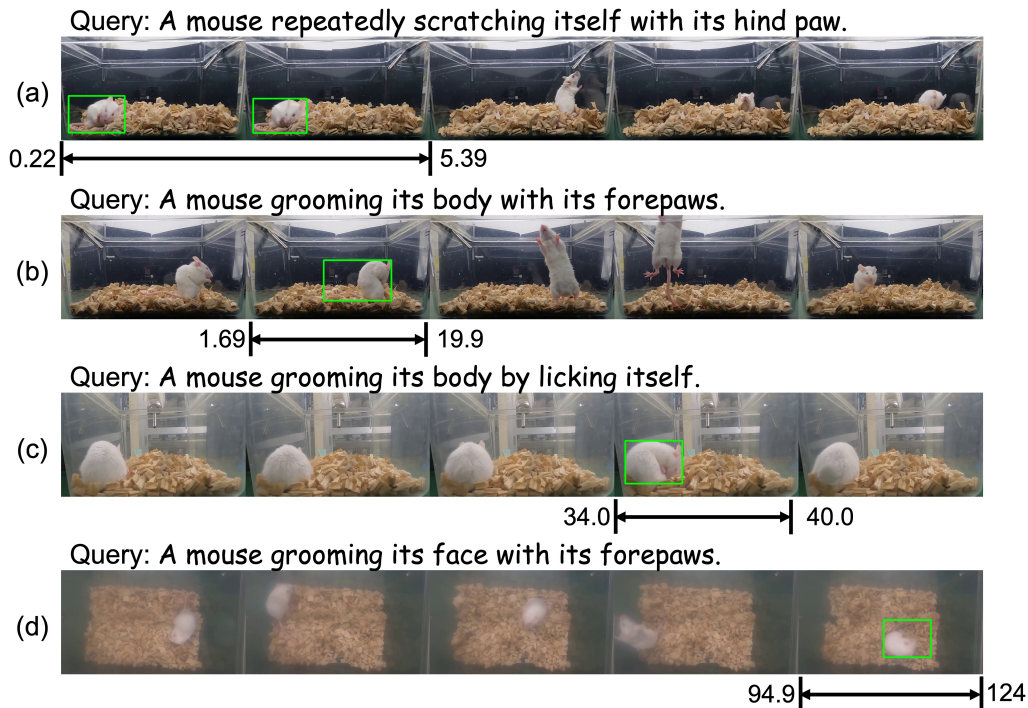


Figure 6: Examples from newly curated Mouse Scratching dataset. The dataset features synchronized four perspectives—(a) Front view 1, (b) Front view 2, (c) Side view, and (d) Top-down spatial view—to capture scratching behaviors in diverse environments. The arrows and numbers (in seconds) in the figure indicate the temporal intervals in which events occur.

Mouse Scratching dataset, illustrating the diversity of behaviors and the four camera perspectives used for annotation. Comprising synchronized four-view video sequences, Mouse Scratching focuses on fine-grained, high-frequency motions—such as distinguishing rapid hind paw scratching from continuous forepaw grooming—that are often difficult to localize in clinical settings. The dataset introduces significant technical challenges, including motion blur and foggy environmental conditions, requiring models to perform robust spatio-temporal reasoning. The annotation schema follows a tripartite logic involving limb identification (hind paw vs. forepaw), target body parts, and action frequency (single vs. repeated), providing a high-fidelity resource for precise behavioral quantification.

MECCANO [44]. MECCANO is an egocentric dataset capturing industrial-like assembly tasks, specifically the construction of a motorbike model. It provides dense annotations for human-object interactions (HOI), including both temporal action segments and spatial bounding boxes for active objects. We leverage these existing HOI labels, specifically utilizing the active object trajectories within their respective interaction windows, to establish the spatio-temporal grounding targets for the industrial domain.

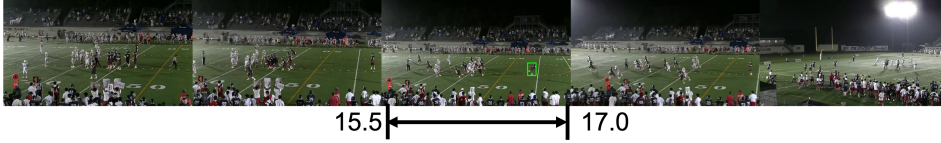
ENIGMA-51 [45]. ENIGMA-51 features egocentric videos of subjects repairing electrical boards using professional tools such as electric screwdrivers and oscilloscopes. While the original dataset provides rich interaction labels, spatial bounding boxes were primarily annotated only at discrete interaction key-frames. To adapt this for STVG, we established continuous spatio-temporal tubes by identifying strict interaction sessions (e.g., from *take* to *release*) and providing dense bounding box annotations for all intermediate frames where they were previously absent. Additionally, we synthesized object-centric natural language queries, such as “the screwdriver being taken,” to serve as the grounding targets. This effort transforms discrete action labels into a dense benchmark for evaluating fine-grained localization in technical industrial workflows.

MultiSports [34]. MultiSports is a large-scale dataset for spatio-temporal action detection, covering 66 fine-grained action classes across four sports: basketball, volleyball, football, and aerobic gymnastics. It is characterized by multi-person scenes with concurrent actions and professional-level competition dynamics. We utilize the original high-quality, 25 fps frame-wise bounding boxes and

Query: A ball carrier takes a handoff and runs with the ball.



Query: A punter receives the snap and kicks the ball downfield.



Query: A kicker kicks the ball from the tee to start or restart play.



Query: A kicker kicks a placed ball toward the goalposts for a field goal attempt.



Query: A receiver catches a forward pass, and the play continues until the receiver is stopped.

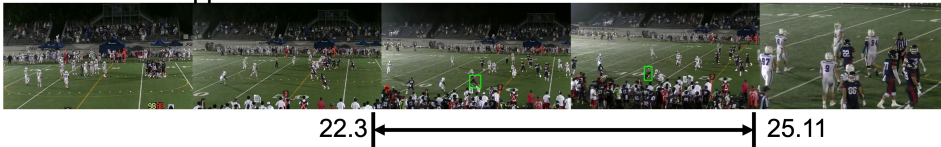


Figure 7: Examples from newly curated American Football dataset. The arrows and numbers (in seconds) in the figure indicate the temporal intervals in which events occur.

temporal labels as the ground truth for our STVG benchmark. This dataset provides a rigorous test for models to handle high-velocity motions and distinguish between subtle, motion-dependent maneuvers in multi-agent environments.

American Football. The American Football dataset, illustrated in [Figure 7](#), is a specialized, expert-grade spatio-temporal grounding benchmark for American Football, newly curated by individuals with years of active playing experience to evaluate tactical execution and athletic performance. Comprising 123 multi-view play sequences totaling over one hour of footage, the dataset focuses on five core action categories—*pass-to-end*, *run-to-end*, *snap-to-punt*, *field-goal*, and *kick-off*—that require precise identification of ball-handling transitions and player roles. The dataset introduces significant technical challenges, including high-speed player collisions, complex occlusions within the line of scrimmage, and varying broadcast perspectives, requiring models to perform robust spatio-temporal reasoning. The annotation schema follows a domain-specific logic that distinguishes nuanced movements, such as the exact moment of a hand-off in running plays, the punter’s reception of the snap, or the specialized mechanics of place-kicking from the tee, providing a high-fidelity resource for automated football analysis and sports coaching.

EgoSurgery [13, 15, 12]. EgoSurgery is a large-scale dataset comprising egocentric open surgery videos captured from head-mounted cameras. It features dense annotations for surgical tools across 15 categories, hand-bounding boxes, and 9 surgical phases. We enriched this dataset for our benchmark by synthesizing textual queries that combine tool identities with their specific surgical context (*e.g.*, "Needle holders during closure"). Characterized by significant tool-shape similarities and heavy

Table 5: Taxonomy of textual queries in the Mouse Scratching dataset.

Behavior	Limb / mode	Target / frequency	Example query
Grooming	licking	body	A mouse grooming its body by licking itself.
Grooming	forepaws	body	A mouse grooming its body with its forepaws.
Grooming	forepaws	face	A mouse grooming its face with its forepaws.
Grooming	forepaws	once	A mouse grooming itself once with its forepaws.
Grooming	forepaws	repeated	A mouse repeatedly grooming itself with its forepaws.
Scratching	hind paw	body	A mouse scratching its body with its hind paw.
Scratching	hind paw	face	A mouse scratching its face with its hind paw.
Scratching	hind paw	once	A mouse scratching itself once with its hind paw.
Scratching	hind paw	repeated	A mouse repeatedly scratching itself with its hind paw.

occlusion by hands and tissues, EgoSurgery provides a highly challenging benchmark for STVG in real-world open surgical environments.

CholecTrack20 [41]. CholecTrack20 is a specialized dataset for multi-class instrument tracking in laparoscopic surgery. While the original dataset provides dense spatial bounding boxes, track IDs, and surgical phases, it does not include natural language descriptions. We enriched this data by generating domain-specific textual queries that link instruments to their operative context (e.g., "Bipolar during gallbladder dissection"). By combining the existing high-quality spatial trajectories with these new queries, we establish a benchmark for STVG in technology-assisted surgical interventions.

UCA [75, 57]. UCA provides fine-grained language descriptions for the UCF-Crime dataset, focusing on various anomalous events in public surveillance scenarios. We utilize the original textual queries and temporal segments as our grounding targets. To enable spatio-temporal evaluation, we supplemented these labels with new spatial bounding box annotations for the entities responsible for the anomalies. This dataset addresses the challenges of low-resolution, exocentric viewpoints typical in urban security monitoring.

DoTA [73]. DoTA is a large-scale egocentric dataset designed for the detection and localization of traffic accidents from a driving perspective. It contains 4,677 video sequences covering 18 anomaly categories, such as vehicle collisions and near-misses. For our benchmark, we utilize the original "when-where" annotations, which provide both the temporal boundaries of the anomalous events and the spatial bounding box tracklets of the involved participants. This dataset serves as a critical testbed for spatio-temporal grounding in highly dynamic, mobile environments characterized by complex ego-motion and rapid incident development.

D Data Collection and Annotation Details for Newly Captured Datasets

We provide additional details for the two newly captured datasets, Mouse Scratching and American Football, because their labels were created specifically for AnyGroundBench. In both cases, the annotation objective was to produce dense spatio-temporal tubes and query descriptions that are faithful to domain-specific event definitions while remaining usable for a unified STVG benchmark.

D.1 Mouse Scratching

Video acquisition and textual query construction. Mouse Scratching videos were recorded in a medical-school environment using four synchronized GoPro cameras. The four-view (two front views, side view, and top-down spatial view) setup was designed to reduce viewpoint ambiguity when distinguishing subtle behaviors around the face and forelimbs. In mouse behavioral analysis [27], forepaw-directed face touching is treated as grooming, whereas hind-paw-directed face touching is treated as scratching, and our annotations follow this distinction. The textual queries were constructed by combining behavior type, contact limb, target region, and repetition pattern, as summarized in Table 5.

Temporal annotation. Temporal ground truth was manually annotated by two medical-school professors who counted facial scratching events. Following their annotation rule, one scratching event was defined from the moment the leg was raised to the moment it was lowered. The temporal

Table 6: Taxonomy of textual queries in the American Football dataset.

Play type	Target role	Example query
Run play	ball carrier	A ball carrier takes a handoff and runs with the ball.
Pass play	receiver	A receiver catches a forward pass, and the play continues until the receiver is stopped.
Punt play	punter	A punter receives the snap and kicks the ball downfield.
Field goal	kicker	A kicker kicks a placed ball toward the goalposts for a field goal attempt.
Kickoff	kicker	A kicker kicks the ball from the tee to start or restart play.

spans were labeled in ELAN, a manual multimodal annotation tool widely used for time-aligned video annotation.

Spatial annotation. For spatial grounding, we used CVAT and created one annotation task for each temporally trimmed ground-truth segment. In each task, we first manually annotated the mouse with a bounding box on the first frame of the segment. We then applied SAM2 tracking to the temporally clipped frames, using the manually specified first-frame bounding box in pixel coordinates as the input prompt. We binarized the SAM2 prediction logits with a threshold of 0 and converted the resulting masks into bounding boxes. As quality control, we visually inspected the bounding boxes and manually corrected segments when clear tracking drift was observed.

D.2 American Football

Video acquisition and textual query construction. The American Football dataset was recorded from university-level amateur games with handheld cameras. Unlike professionally produced broadcast footage, these videos reflect real-world amateur recording conditions and often contain spectators and other non-player distractors in the scene. The textual queries were constructed with an experienced American football player so that the linguistic descriptions were natural in the context of American football gameplay and aligned with football-specific event definitions. The textual queries were organized around football-specific play outcomes and target roles, as summarized in Table 6.

Temporal annotation. Temporal annotations were created by an annotator with several years of American football playing experience. The videos were examined frame by frame at 30 fps to identify the start and end frames of each target event, and both the frame indices and their corresponding timestamps in seconds were recorded.

Spatial annotation. For kick plays and pass plays, we first clipped the video to the annotated temporal interval, manually drew a bounding box on the first frame, and then tracked the target with the Ultralytics SAM3VideoPredictor. The inputs to the tracker were the temporally clipped video and the manually annotated first-frame bounding box. The model outputs both masks and bounding boxes, and we extracted the predicted spatial extent from the pixels with mask values greater than zero. As quality control, segments with visible drift were manually corrected by additional bounding-box annotation. For run plays, however, player density and severe occlusion made off-the-shelf tracking unreliable, so these segments were annotated fully by hand in CVAT.

E Licenses and Redistribution Constraints

For curated benchmark components derived from existing datasets, each component remains subject to the license and terms of use of its source dataset. Our release does not redistribute the original videos for these components; instead, users must obtain the source videos from the official dataset providers and comply with the corresponding source licenses. We release the curated benchmark metadata needed for evaluation, including query definitions, splits, and derived grounding annotations where applicable. For the newly captured Mouse Scratching and American Football datasets, we release the data under CC BY-NC-SA 4.0.

- **Animal Kingdom**⁵: available through a dataset-use questionnaire. We filled out the questionnaire and obtained an official download link. We also emailed the authors about our use of the dataset in this paper.
- **Mouse Scratching**: newly captured dataset released under CC BY-NC-SA 4.0.

⁵Official repository: <https://github.com/sutdvc/Animal-Kingdom>.

- **MECCANO**⁶: publicly available through the official provider.
- **ENIGMA-51**⁷: publicly available through the official provider.
- **American Football**: newly captured dataset released under CC BY-NC-SA 4.0.
- **MultiSports**⁸: CC BY-NC 4.0; users should obtain the source dataset from the official provider and comply with the non-commercial license terms.
- **CholecTrack20**⁹: CC BY-NC-SA 4.0 and subject to the provider’s data-use agreement; users should obtain the source dataset through the official access process.
- **UCA annotations**¹⁰: Apache-2.0, with academic/research-use restrictions stated by the dataset provider; the underlying UCF-Crime [57] videos must be obtained separately from the original provider.
- **DoTA**¹¹: MIT; users should obtain the source dataset from the official provider and comply with any terms governing the released video clips and annotations.
- **EgoSurgery**¹²: CC BY-NC-SA 4.0, limited by the provider to academic research and non-commercial use; users must obtain access through the official request process.

F Main Results under Stricter Evaluation Metrics

We provide comprehensive evaluation results on our benchmark under stricter IoU thresholds. Specifically, for STVG, following previous works [70, 56, 26], we evaluate the performance using m_t IoU, m_v IoU, and v IoU@0.5. For TVG, consistent with established conventions [48, 24], we report t IoU@0.5, t IoU@0.7, and m_t IoU. For SVG, we also report m_s IoU and s IoU@0.5. Table 7, Table 8, and Table 9 provide the corresponding supplementary results for STVG, TVG, and SVG, respectively. These tables complement the main results by showing whether the observed model rankings and ICL trends remain stable under stricter or more detailed evaluation metrics.

G Further Analysis

G.1 Observation from Main Table

Domain-wise Performance Patterns. The five domains exhibit markedly different difficulty profiles in the main table. Based on the zero-shot averages, Animal is the easiest domain for STVG, whereas Surgery and Sports are the most difficult. Public Security is the clearest exception on TVG, reaching by far the highest temporal average and the highest best-case score, while Sports remains weak across tasks. The task gaps further sharpen this contrast: Public Security shows the largest TVG–STVG gap, indicating that temporal localization can be relatively strong even when full grounding remains difficult, whereas Sports stays low even after decomposition into TVG and SVG.

ICL is also highly domain-dependent. On average, Surgery and Public Security benefit the most from 2-shot prompting, especially on TVG, whereas Animal shows little or negative improvement across tasks. The best proprietary–OSS gap is likewise largest in Public Security, while Sports remains low even for the strongest proprietary models, suggesting a domain-level difficulty that is not confined to a single model family.

Spatio-Temporal Video Grounding. Full spatio-temporal grounding remains unresolved across the five specialized domains. For example, Gemini-3.1-Pro, the strongest proprietary model in our benchmark, reaches only 22.8 on Public Security and 16.5 on Animal, while dropping to 1.22 on Sports in the zero-shot setting. Even this strongest model does not achieve consistently strong STVG performance across the benchmark, and its gains remain highly uneven across domains. This pattern indicates that partial success in some settings does not translate into robust specialized-domain tube

⁶Official repository: <https://github.com/fpv-iplab/MECCANO>.

⁷Official repository: <https://github.com/fpv-iplab/ENIGMA-51>.

⁸Official repository: <https://github.com/MCG-NJU/MultiSports>.

⁹Official repository: <https://github.com/CAMMA-public/cholectrack20>.

¹⁰Official repository: <https://github.com/Xuange923/Surveillance-Video-Understanding>.

¹¹Official repository: <https://github.com/MoonBlvd/Detection-of-Traffic-Anomaly>.

¹²Official repository: <https://github.com/Fujiry0/EgoSurgery>.

Table 7: Additional results of MLLMs on the Spatio-Temporal Video Grounding task in Any-GroundBench. Each cell reports m_t IoU / m_v IoU / v IoU@0.5. For each model, the first row shows the zero-shot baseline, and the second row (shaded, +ICL) shows the performance with 2-shot In-Context Learning; purple and red scores denote performance improvements and degradations relative to the zero-shot baseline, respectively. †Text-only baseline used Gemini-3.1-Pro without video inputs.

Models	Animal	Industry	Sports	Surgery	Public Security
Text-only†	13.2 / 1.58 / 0.00	7.79 / 1.55 / 0.59	11.6 / 0.28 / 0.00	8.77 / 0.67 / 0.00	32.7 / 2.38 / 0.00
+ICL	12.9 / 1.85 / 0.00	6.55 / 1.75 / 0.59	19.8 / 0.29 / 0.00	11.4 / 1.75 / 0.00	38.5 / 4.01 / 0.00
<i>Proprietary MLLMs</i>					
GPT-4o	9.70 / 1.58 / 0.00	10.7 / 2.55 / 0.59	18.8 / 0.77 / 0.00	10.9 / 1.10 / 0.00	28.1 / 4.89 / 0.00
+ICL	10.5 / 2.11 / 0.00	5.65 / 0.97 / 0.20	26.3 / 1.20 / 0.00	19.9 / 2.26 / 0.00	44.1 / 8.59 / 0.00
GPT-5.1	18.0 / 4.96 / 0.00	10.9 / 4.10 / 2.36	13.5 / 0.63 / 0.00	14.1 / 2.54 / 0.00	38.8 / 9.47 / 0.80
+ICL	19.7 / 7.76 / 1.84	6.83 / 2.23 / 0.54	26.9 / 1.50 / 0.61	24.4 / 4.95 / 0.00	43.0 / 11.3 / 0.80
Gemini-2.5-Flash	14.8 / 4.44 / 0.63	14.3 / 1.01 / 0.00	32.6 / 1.72 / 1.22	14.8 / 1.26 / 0.00	25.9 / 3.98 / 0.00
+ICL	15.6 / 3.31 / 0.00	11.1 / 1.22 / 0.00	33.6 / 1.21 / 0.00	11.3 / 0.96 / 0.00	32.8 / 5.18 / 0.00
Gemini-2.5-Pro	23.5 / 8.44 / 3.18	21.8 / 1.92 / 0.00	35.3 / 2.17 / 0.61	22.6 / 3.66 / 0.00	40.5 / 8.66 / 0.80
+ICL	24.5 / 9.02 / 3.82	26.8 / 5.85 / 3.55	38.7 / 4.65 / 1.22	30.8 / 7.07 / 0.46	41.6 / 10.0 / 1.20
Gemini-3-Flash	28.4 / 12.2 / 5.73	14.8 / 4.90 / 2.36	32.6 / 2.78 / 0.00	11.3 / 2.91 / 0.00	37.6 / 12.8 / 1.20
+ICL	28.3 / 12.1 / 4.45	18.0 / 5.76 / 2.95	28.3 / 1.54 / 0.00	20.6 / 6.93 / 1.85	46.2 / 20.5 / 8.80
Gemini-3.1-Pro	29.0 / 12.9 / 6.36	19.6 / 6.22 / 2.36	31.2 / 3.26 / 0.00	18.9 / 6.54 / 0.46	40.4 / 17.0 / 4.40
+ICL	26.6 / 10.9 / 6.36	20.3 / 8.37 / 5.91	22.7 / 1.51 / 0.00	19.8 / 6.93 / 4.16	42.8 / 17.8 / 6.80
<i>Open-source Specialized MLLMs</i>					
LLaVA-ST	17.4 / 7.85 / 2.54	3.67 / 0.77 / 0.00	15.5 / 0.66 / 0.00	7.08 / 0.57 / 0.00	32.4 / 3.97 / 0.00
<i>Open-source General-Purpose MLLMs</i>					
Qwen3-VL-4B	16.4 / 6.28 / 1.27	6.13 / 0.57 / 0.00	10.9 / 0.06 / 0.00	11.5 / 0.94 / 0.00	22.4 / 2.20 / 0.00
+ICL	1.03 / 0.39 / 0.00	1.00 / 0.48 / 0.00	0.30 / 0.00 / 0.00	0.99 / 0.08 / 0.00	0.36 / 0.00 / 0.00
Qwen3-VL-8B	18.7 / 4.76 / 1.27	6.76 / 0.81 / 0.00	11.7 / 0.02 / 0.00	10.3 / 0.77 / 0.00	27.6 / 2.27 / 0.00
+ICL	2.23 / 0.54 / 0.00	1.10 / 0.66 / 0.59	3.82 / 0.01 / 0.00	1.15 / 0.13 / 0.00	1.92 / 0.55 / 0.00
Qwen3.5-4B	24.0 / 4.28 / 0.63	10.8 / 0.45 / 0.00	15.2 / 0.13 / 0.00	13.3 / 0.65 / 0.00	31.6 / 1.56 / 0.00
+ICL	20.4 / 4.18 / 0.00	10.4 / 2.35 / 0.59	13.1 / 0.14 / 0.00	13.1 / 1.78 / 0.00	33.9 / 4.08 / 0.40
Qwen3.5-9B	24.6 / 4.33 / 0.63	9.04 / 1.06 / 0.00	14.1 / 0.22 / 0.00	13.1 / 0.73 / 0.00	32.1 / 1.31 / 0.00
+ICL	22.1 / 3.75 / 0.63	8.08 / 1.78 / 0.00	17.3 / 0.25 / 0.00	11.0 / 1.55 / 0.00	33.1 / 3.41 / 0.00
Eagle2.5-8B	3.62 / 0.45 / 0.00	5.64 / 0.25 / 0.00	2.76 / 0.03 / 0.00	3.10 / 0.18 / 0.00	10.4 / 0.72 / 0.00
+ICL	1.56 / 0.18 / 0.00	0.00 / 0.00 / 0.00	0.00 / 0.00 / 0.00	1.00 / 0.12 / 0.00	0.00 / 0.00 / 0.00
InternVL3-8B	10.9 / 1.03 / 0.00	3.69 / 0.19 / 0.00	4.13 / 0.00 / 0.00	6.29 / 0.19 / 0.00	6.99 / 0.30 / 0.00
+ICL	0.85 / 0.18 / 0.00	0.46 / 0.15 / 0.00	0.00 / 0.00 / 0.00	0.02 / 0.00 / 0.00	0.03 / 0.00 / 0.00
InternVL3-14B	14.1 / 1.88 / 0.00	3.37 / 0.12 / 0.00	12.2 / 0.01 / 0.00	7.55 / 0.17 / 0.00	22.7 / 0.74 / 0.00
+ICL	3.68 / 0.61 / 0.00	0.45 / 0.06 / 0.00	0.51 / 0.00 / 0.00	1.84 / 0.06 / 0.00	0.35 / 0.01 / 0.00
InternVL3.5-8B	15.5 / 0.33 / 0.00	5.52 / 0.02 / 0.00	7.64 / 0.00 / 0.00	5.88 / 0.13 / 0.00	13.0 / 0.05 / 0.00
+ICL	2.01 / 0.17 / 0.00	0.15 / 0.01 / 0.00	3.73 / 0.03 / 0.00	1.57 / 0.25 / 0.00	15.9 / 1.32 / 0.00

grounding overall. ICL also does not provide a reliable remedy: for example, GPT-5.1 improves from 4.8 to 9.63 on Public Security, but Gemini-3.1-Pro drops from 16.5 to 12.7 on Animal, and the stronger open-source Qwen3.5-9B also drops from 4.45 to 2.54 on Animal. These results suggest that simple inference-time adaptation is insufficient for specialized-domain STVG, motivating a closer diagnosis through the decomposed TVG and SVG results.

Spatial Video Grounding. Across most domains, SVG scores remain substantially higher than the corresponding STVG scores. For example, Gemini-3.1-Pro improves from 16.5 to 70.7 on Animal, from 7.69 to 41.4 on Industry, from 4.16 to 26.1 on Surgery, and from 22.8 to 52.0 on Public Security when moving from STVG to SVG. These large gaps show that full spatio-temporal grounding often breaks down even after the target can be localized reasonably well within a trimmed temporal window. ICL is also unstable for SVG: GPT-4o drops from 14.7 to 4.14 on Industry, Gemini-3.1-Pro drops from 52.0 to 41.6 on Public Security, and the stronger open-source Qwen3.5-9B drops from 20.3 to 10.1 on Animal.

Temporal Video Grounding. Temporal grounding is comparatively more tractable than full spatio-temporal grounding, but it remains far from solved in specialized domains. Across most domains, the best zero-shot TVG scores are substantially higher than the corresponding STVG scores, although the absolute performance remains limited outside Public Security: the strongest zero-shot results reach

Table 8: Additional results of MLLMs on the Temporal Video Grounding task in AnyGroundBench. Each cell reports $tIoU@0.5$ / $tIoU@0.7$ / $mIoU$. For each model, the first row shows the zero-shot baseline, and the second row (shaded, +ICL) shows the performance with 2-shot In-Context Learning; purple scores denote performance improvements or ties and red scores denote degradations relative to the zero-shot baseline. †Text-only baseline used Gemini-3.1-Pro without video inputs.

Models	Animal	Industry	Sports	Surgery	Public Security
Text-only†	8.28 / 3.18 / 14.4	3.55 / 0.59 / 4.92	1.84 / 0.00 / 8.21	9.72 / 2.31 / 15.2	18.0 / 6.40 / 32.7
+ICL	8.91 / 3.82 / 13.2	5.32 / 0.59 / 5.80	5.52 / 1.84 / 11.7	12.9 / 4.16 / 18.6	35.2 / 15.2 / 39.7
<i>Proprietary MLLMs</i>					
GPT-4o	9.55 / 5.09 / 11.8	5.91 / 4.14 / 6.92	6.74 / 2.45 / 13.7	8.79 / 3.24 / 10.7	27.2 / 6.80 / 33.9
+ICL	8.69 / 1.73 / 10.6	7.82 / 1.73 / 7.57	11.6 / 5.52 / 15.2	13.3 / 4.44 / 17.1	34.3 / 11.0 / 38.7
GPT-5.1	12.7 / 7.00 / 14.0	6.50 / 3.55 / 6.21	12.2 / 3.06 / 18.4	18.0 / 9.25 / 17.0	34.4 / 12.8 / 38.5
+ICL	14.4 / 7.89 / 17.0	6.81 / 3.03 / 8.52	9.81 / 2.45 / 17.7	29.1 / 13.2 / 29.4	36.8 / 14.8 / 40.6
Gemini-2.5-Flash	20.3 / 13.3 / 20.8	10.6 / 4.73 / 14.6	14.1 / 4.29 / 19.8	14.8 / 8.33 / 17.9	28.4 / 9.60 / 31.2
+ICL	13.3 / 6.36 / 14.4	13.6 / 6.50 / 14.6	27.6 / 12.2 / 27.0	14.3 / 6.94 / 15.5	38.0 / 12.0 / 39.4
Gemini-2.5-Pro	26.1 / 13.3 / 26.5	26.6 / 11.8 / 26.7	22.6 / 5.52 / 25.6	22.6 / 15.7 / 25.0	40.9 / 16.0 / 41.5
+ICL	21.6 / 14.6 / 22.5	27.2 / 12.4 / 24.4	31.2 / 13.4 / 30.1	27.7 / 17.5 / 30.6	41.2 / 16.0 / 42.2
Gemini-3-Flash	24.8 / 15.9 / 28.4	16.5 / 8.28 / 20.9	15.3 / 6.13 / 22.4	30.5 / 20.8 / 30.0	38.8 / 10.4 / 40.7
+ICL	22.9 / 11.4 / 23.3	23.6 / 8.87 / 21.4	26.9 / 9.20 / 28.1	31.0 / 19.4 / 31.5	52.0 / 23.2 / 49.3
Gemini-3.1-Pro	24.8 / 15.9 / 26.4	13.0 / 8.87 / 18.4	10.4 / 3.06 / 19.2	23.1 / 14.3 / 25.4	38.9 / 12.8 / 41.2
+ICL	23.5 / 14.0 / 24.8	15.9 / 8.87 / 20.5	20.2 / 7.97 / 25.8	28.7 / 18.5 / 31.0	50.0 / 19.6 / 47.9
<i>Open-source Specialized MLLMs</i>					
LLaVA-ST	14.6 / 8.28 / 15.8	4.73 / 0.59 / 6.55	1.84 / 0.61 / 6.27	5.09 / 2.77 / 9.50	17.6 / 5.20 / 24.3
<i>Open-source General-Purpose MLLMs</i>					
Qwen3-VL-4B	15.9 / 10.8 / 18.8	3.55 / 1.18 / 5.13	3.68 / 0.61 / 10.5	6.48 / 4.16 / 10.7	12.0 / 4.00 / 24.8
+ICL	18.4 / 10.8 / 21.3	8.87 / 5.91 / 12.0	11.0 / 3.68 / 13.6	22.2 / 12.0 / 25.3	37.6 / 12.8 / 38.4
Qwen3-VL-8B	11.4 / 5.73 / 14.1	5.91 / 0.59 / 8.33	1.22 / 0.00 / 10.5	5.09 / 3.70 / 10.6	16.0 / 2.00 / 29.4
+ICL	19.7 / 8.91 / 20.7	8.28 / 3.55 / 10.6	14.7 / 2.45 / 16.4	18.0 / 10.6 / 24.2	37.6 / 12.0 / 39.0
Qwen3.5-4B	21.0 / 12.7 / 24.5	10.0 / 2.36 / 12.5	4.90 / 0.00 / 12.2	16.6 / 10.1 / 19.9	17.2 / 4.80 / 32.2
+ICL	18.4 / 8.91 / 20.7	14.7 / 8.87 / 15.8	10.4 / 1.84 / 14.5	22.2 / 12.9 / 24.3	39.6 / 15.6 / 41.7
Qwen3.5-9B	24.2 / 15.2 / 27.3	7.69 / 1.18 / 12.4	4.90 / 0.00 / 13.0	21.2 / 17.5 / 23.5	16.0 / 5.20 / 32.9
+ICL	22.9 / 10.8 / 23.7	13.6 / 7.69 / 13.7	13.4 / 4.90 / 17.1	15.7 / 11.1 / 19.7	37.6 / 14.0 / 39.2
Eagle2.5-8B	14.0 / 7.00 / 16.3	2.95 / 1.18 / 5.12	3.68 / 0.00 / 9.40	8.33 / 3.24 / 10.2	20.8 / 5.60 / 29.2
+ICL	15.9 / 5.73 / 17.1	8.87 / 5.32 / 9.31	8.58 / 3.68 / 12.6	15.7 / 8.33 / 19.5	38.0 / 12.0 / 38.6
InternVL3-8B	8.91 / 3.82 / 11.7	2.36 / 1.18 / 4.75	2.46 / 0.00 / 7.85	3.70 / 1.38 / 8.60	2.00 / 0.40 / 3.41
+ICL	7.00 / 1.27 / 10.5	3.55 / 1.18 / 4.54	4.90 / 1.84 / 6.34	7.87 / 2.77 / 16.4	1.20 / 0.80 / 5.23
InternVL3-14B	5.73 / 3.18 / 12.6	1.18 / 0.59 / 3.58	3.06 / 0.00 / 7.37	3.70 / 0.46 / 8.40	5.20 / 2.80 / 8.70
+ICL	11.8 / 4.23 / 11.4	3.12 / 0.78 / 4.90	6.17 / 1.23 / 6.04	2.79 / 1.11 / 10.0	8.67 / 2.89 / 11.9
InternVL3.5-8B	7.64 / 1.27 / 9.53	1.18 / 0.00 / 4.05	3.68 / 1.84 / 4.49	2.77 / 0.92 / 7.07	1.60 / 0.80 / 2.02
+ICL	2.54 / 0.63 / 3.78	3.12 / 1.56 / 4.49	2.45 / 1.22 / 3.34	7.40 / 2.77 / 10.8	3.20 / 1.60 / 2.81

37.5 on Animal, 39.6 on Industry, 37.4 on Sports, 37.9 on Surgery, and 69.4 on Public Security. This gap suggests that current MLLMs can often infer when an event occurs before they can accurately ground it as a spatio-temporal tube.

ICL also tends to help TVG more consistently than STVG or SVG. For example, GPT-5.1 improves from 22.6 to 41.7 on Surgery, and Gemini-3-Flash improves from 66.8 to 78.4 on Public Security. However, these gains still do not translate into reliable STVG, indicating that specialized-domain failures cannot be explained by temporal errors alone.

G.2 Threshold Sensitivity Analysis

Figure 8 shows how representative models behave as the IoU threshold is varied from 0.1 to 0.9. Across models, STVG accuracy decreases sharply as the threshold becomes stricter. Gemini-3.1-Pro remains the strongest model over most thresholds, but even its STVG curve falls rapidly from the permissive regime to nearly zero at high thresholds. TVG degrades more gradually than STVG and SVG, which reinforces the main-table observation that temporal localization is comparatively more robust than precise tube grounding.

Figure 9 presents the same analysis aggregated by domain for Gemini-3.1-Pro. Animal and Public Security remain the strongest domains under loose thresholds, whereas Sports and Surgery are

Table 9: Additional results of MLLMs on the Spatial Video Grounding task in AnyGroundBench. Each cell reports $m_s\text{IoU} / s\text{IoU}@0.5$. For each model, the first row shows the zero-shot baseline, and the second row (shaded, +ICL) shows the performance with 2-shot In-Context Learning; purple and red scores denote performance improvements and degradations relative to the zero-shot baseline, respectively. †Text-only baseline used Gemini-3.1-Pro without video inputs.

Models	Animal	Industry	Sports	Surgery	Public Security
Text-only†	2.54 / 12.8	0.59 / 5.95	0.00 / 2.48	0.00 / 3.56	0.00 / 4.74
+ICL	3.82 / 12.9	2.95 / 9.72	0.00 / 0.67	0.92 / 10.0	0.00 / 3.95
<i>Proprietary MLLMs</i>					
GPT-4o	1.91 / 7.89	2.95 / 9.75	0.00 / 0.62	0.00 / 1.74	1.60 / 6.56
+ICL	2.54 / 9.86	1.18 / 3.21	0.00 / 0.68	0.00 / 2.22	2.00 / 6.60
GPT-5.1	22.9 / 30.7	14.7 / 17.7	1.22 / 1.78	0.00 / 4.91	11.9 / 22.6
+ICL	31.8 / 36.1	19.5 / 21.6	2.45 / 5.29	0.00 / 5.42	11.5 / 24.9
Gemini-2.5-Flash	5.73 / 12.6	2.95 / 4.17	2.45 / 2.80	0.00 / 3.43	0.00 / 3.06
+ICL	1.91 / 9.76	3.55 / 7.64	0.00 / 1.06	0.89 / 3.69	0.80 / 6.43
Gemini-2.5-Pro	9.55 / 14.0	10.0 / 14.2	4.29 / 5.90	0.00 / 2.79	10.0 / 15.8
+ICL	29.9 / 29.7	14.7 / 17.3	3.06 / 5.04	9.89 / 15.9	8.40 / 14.7
Gemini-3-Flash	36.9 / 37.1	10.6 / 15.6	1.84 / 4.17	1.49 / 10.1	22.7 / 29.7
+ICL	30.5 / 31.8	15.9 / 17.4	1.84 / 2.77	15.3 / 18.1	11.5 / 15.3
Gemini-3.1-Pro	49.0 / 49.1	31.9 / 31.0	7.97 / 13.1	2.53 / 15.4	28.4 / 33.1
+ICL	42.6 / 41.8	32.5 / 29.5	5.52 / 6.89	9.52 / 16.5	21.2 / 26.3
<i>Open-source Specialized MLLMs</i>					
LLaVA-ST	23.5 / 32.2	5.32 / 10.7	1.84 / 4.68	0.00 / 4.35	2.40 / 13.8
<i>Open-source General-Purpose MLLMs</i>					
Qwen3-VL-4B	5.73 / 16.1	0.59 / 3.49	0.00 / 0.07	0.00 / 0.95	0.00 / 3.86
+ICL	0.00 / 0.98	0.00 / 0.11	0.00 / 0.00	0.00 / 0.19	0.00 / 0.16
Qwen3-VL-8B	0.00 / 0.00	0.00 / 0.00	0.00 / 0.00	0.00 / 0.00	0.00 / 0.00
+ICL	1.27 / 3.88	0.00 / 0.00	0.00 / 0.09	0.00 / 0.75	0.00 / 0.09
Qwen3.5-4B	3.18 / 13.1	2.36 / 6.96	0.00 / 0.11	0.00 / 2.81	0.40 / 2.25
+ICL	3.18 / 13.3	1.18 / 6.63	0.00 / 0.45	0.89 / 6.67	0.80 / 4.64
Qwen3.5-9B	7.00 / 17.3	1.18 / 8.79	0.00 / 0.13	0.00 / 4.12	0.80 / 5.09
+ICL	1.91 / 10.0	2.36 / 9.44	0.00 / 0.66	1.34 / 6.91	0.40 / 3.89
Eagle2.5-8B	0.00 / 1.32	0.00 / 1.90	0.00 / 0.05	0.00 / 0.56	0.00 / 0.33
+ICL	0.00 / 0.50	0.00 / 0.18	0.00 / 0.00	0.00 / 0.62	0.00 / 0.00
InternVL3-8B	0.00 / 4.63	0.00 / 1.25	0.00 / 0.00	0.00 / 0.54	0.00 / 0.61
+ICL	0.00 / 0.26	0.00 / 0.12	0.00 / 0.00	0.00 / 0.10	0.00 / 0.02
InternVL3-14B	1.91 / 7.73	0.00 / 2.05	0.00 / 0.00	0.00 / 0.70	0.00 / 0.57
+ICL	0.00 / 1.39	0.00 / 0.11	0.00 / 0.03	0.00 / 0.31	0.00 / 0.30
InternVL3.5-8B	0.00 / 1.34	0.00 / 0.81	0.00 / 0.00	0.00 / 0.45	0.00 / 0.20
+ICL	0.00 / 1.57	0.59 / 1.96	0.00 / 0.01	0.44 / 4.08	0.00 / 0.12

consistently difficult. However, all domains show a steep decline in STVG as the threshold increases. This indicates that domain-specific STVG failures are not only ranking artifacts at a single threshold; they reflect a broader lack of precise spatio-temporal overlap.

G.3 Prompt Sensitivity to Bounding-Box Coordinate Order

We further analyze Gemini-3.1-Pro’s sensitivity to the requested bounding-box coordinate order in STVG. Table 10 compares zero-shot outputs generated with either yxyx or xyxy prompts, and then parses each output under both coordinate-order assumptions. The main pattern is consistent: both prompt variants achieve much higher spatial and volume scores when the predicted boxes are parsed as yxyx. For example, the corrected yxyx prompt obtains 9.77 $m_v\text{IoU}$ under yxyx parsing but only

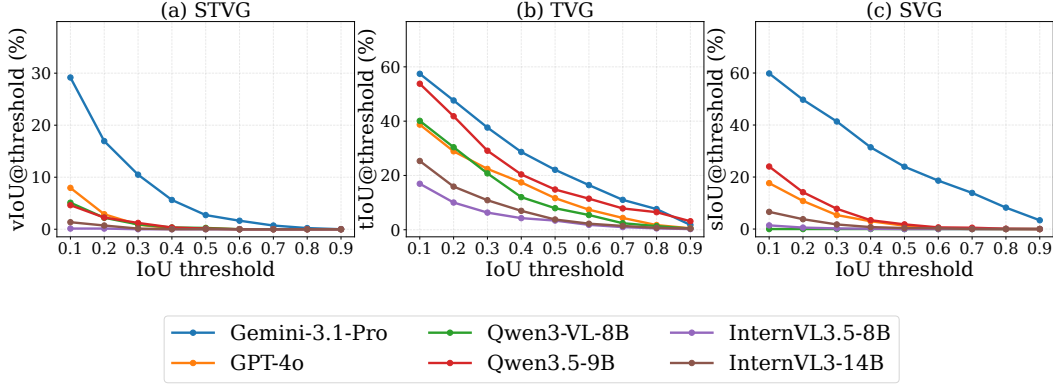


Figure 8: **Model-wise threshold sensitivity across STVG, TVG, and SVG.** Each curve reports the percentage of examples above each IoU threshold. STVG and SVG use $vIoU$ and $sIoU$ thresholds, respectively, while TVG uses temporal IoU thresholds. STVG accuracy drops sharply as the threshold increases, showing that coarse success at permissive thresholds rarely becomes precise tube grounding.

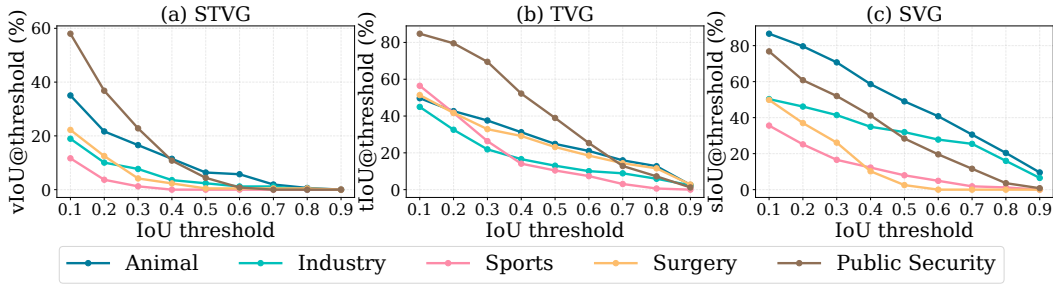


Figure 9: **Domain-wise threshold sensitivity for Gemini-3.1-Pro.** Each curve aggregates results within one domain across STVG, TVG, and SVG. Public Security and Animal remain relatively strong at loose thresholds, while Sports and Surgery are consistently difficult. Across all domains, STVG degrades much more sharply than TVG, confirming that precise spatio-temporal overlap is the central failure mode.

3.25 under $xyxy$ parsing, while the older $xyxy$ prompt similarly improves from 3.31 to 9.72 when parsed as $yxyx$.

This suggests that Gemini-3.1-Pro tends to follow its native `box_2d` convention, *i.e.*, $[y_{min}, x_{min}, y_{max}, x_{max}]$, even when the prompt requests $xyxy$. The temporal metric is nearly unchanged because coordinate order does not affect the predicted temporal interval, whereas spatial overlap, tube precision, and tube recall collapse when the boxes are parsed with the wrong x/y convention. Although the $xyxy$ and $yxyx$ prompt outputs were generated in separate runs, the large gap from re-parsing the same outputs and the consistent domain-wise trend indicate that Gemini’s coordinate-order convention is the dominant factor.

H Limitations and Future Work

Task Scope. AnyGroundBench centers on single-query grounding: each query is generated from a single target object tube and its bounding boxes. This design supports diagnosis of spatial and temporal localization failures, but not open-ended expert QA, causal reasoning, or multi-object relational understanding. Extensions to multi-query, multi-object, and instruction-following settings would cover other aspects of specialized video workflows.

Video Length. AnyGroundBench uses short clips to support dense tube annotation and broad MLLM evaluation. The average video is 47.13s and the average target segment is 7.51s, so the benchmark does not test long-form video search. Extensions to longer videos would require coarse-to-fine retrieval, adaptive frame selection, and memory over sparse events.

Table 10: **Prompt sensitivity to bounding-box coordinate order for Gemini-3.1-Pro on STVG.** We compare zero-shot outputs generated with *yxyx* and *xyxy* prompts, and evaluate each output under both parsing assumptions. “Prompted order” denotes the coordinate order explicitly requested in the prompt, while “parsed order” denotes the coordinate order assumed when converting Gemini’s raw predicted boxes before evaluation.

Prompted order	Parsed order	m_t IoU	m_v IoU	v Precision	v Recall
<i>yxyx</i>	<i>yxyx</i>	28.47	9.77	11.36	19.76
<i>yxyx</i>	<i>xyxy</i>	28.47	3.25	3.87	6.74
<i>xyxy</i>	<i>xyxy</i>	28.81	3.31	3.88	6.81
<i>xyxy</i>	<i>yxyx</i>	28.81	9.72	11.27	19.78